
This is an electronic reprint of the original article.
This reprint may differ from the original in pagination and typographic detail.

Al-Juboori, Raed A.; Uzkurt Kaljunen, Juho; Righetto, Ilaria; Mikola, Anna

Membrane contactor onsite piloting for nutrient recovery from mesophilic digester reject water : The effect of process conditions and pre-treatment options

Published in:
Separation and Purification Technology

DOI:
[10.1016/j.seppur.2022.122250](https://doi.org/10.1016/j.seppur.2022.122250)

Published: 15/12/2022

Document Version
Publisher's PDF, also known as Version of record

Published under the following license:
CC BY-NC-ND

Please cite the original version:
Al-Juboori, R. A., Uzkurt Kaljunen, J., Righetto, I., & Mikola, A. (2022). Membrane contactor onsite piloting for nutrient recovery from mesophilic digester reject water : The effect of process conditions and pre-treatment options. *Separation and Purification Technology*, 303, Article 122250.
<https://doi.org/10.1016/j.seppur.2022.122250>

This material is protected by copyright and other intellectual property rights, and duplication or sale of all or part of any of the repository collections is not permitted, except that material may be duplicated by you for your research use or educational purposes in electronic or print form. You must obtain permission for any other use. Electronic or print copies may not be offered, whether for sale or otherwise to anyone who is not an authorised user.



Membrane contactor onsite piloting for nutrient recovery from mesophilic digester reject water: The effect of process conditions and pre-treatment options

Raed A. Al-Juboori^{a,b,*}, Juho Uzkuurt Kaljunen^a, Ilaria Righetto^{a,c}, Anna Mikola^a

^a Water and Environmental Engineering Research Group, Department of Built Environment, Aalto University, P.O. Box 15200, Aalto, FI-00076 Espoo, Finland

^b NYUAD Water Research Center, New York University-Abu Dhabi Campus, P.O. Box 129188, Abu Dhabi, United Arab Emirates

^c Department of Environment, Land and Infrastructure Engineering, Politecnico di Torino, Corso Duca Degli Abruzzi, 24, 10129 Torino, Italy

ARTICLE INFO

Keywords:

Nitrogen recovery
Phosphorous removal
Mesophilic digester
Membrane contactor
Pre-treatment
Starch

ABSTRACT

Nutrient recovery is an important segment of the circular economy, and it significantly contributes to sustainable development goals. This work reports on the outcomes of a field testing pilot-scale membrane contactor system designed for nitrogen (N) and phosphorous (P) recovery in the form of high purity ammonium salts and high-quality P containing sludge. The pilot testing was conducted at the Viikinmäki WWTP using digester reject water under different treatment conditions. Our system showed a high tolerance for solids (concentration > 500 mg/L). Field test trials showed that the higher the feed flow, the better the ammonia transfer rate. Decreasing the retention time from 4 h to 2 h increased the ammonia mass transfer rate constant by >150 %. Among the tested feed pH levels, a pH of 10 had the highest solids removal, which in turn resulted in the highest ammonia recovery percentage. A high acid concentration lowered the ammonia transfer rate. Strong acids such as HNO₃ and H₂SO₄ had a higher ammonia recovery than that of H₃PO₄. Pre-treating feedwater with starch resulted in the same ammonia accumulation rate as a poly-aluminum chloride (PAX)/polymer pre-treatment. The highest PO₄³⁻ removal of 99 % was achieved with a PAX/polymer treatment at pH 10, whereas the highest total phosphorous removal of 77 % was achieved with a starch treatment. The produced sludge consists mainly of CaCO₃ emanating from the used lime, which can be used as a soil amendment. The produced ammonium salts were of high purity and have a nutrient content comparable to that of commercial fertilizers. This study provides important insights into the selection of process parameters of membrane contactor systems based on the goal of the treatment, whether it be nutrient removal or recovery.

1. Introduction

The main daunting challenges that face our world today are the projected population growth, the depleting resources, and the deteriorating environment. The world's population is expected to increase to 9.73 billion by 2050, and this necessitates an increase in agricultural output by at least one-third [1]. The increase in population would be accompanied by a rise in urbanization and the loss of agricultural land [1]. This means an increase in production with less land, which in turn increases demands on fertilizers. The main elements that fertilizers provide to plants are nitrogen and phosphorous. Nitrogen fertilizers are currently produced through the Haber-Bosch process [2]. Haber-Bosch is an energy-intensive process that consumes about 1–2 % of global energy [3]. Similarly, phosphorous fertilizers are largely dependent on

the mining of phosphorous rocks. The natural reserves of phosphorous are prone to depletion [4]. Based on the static lifetime assumption for P reserves, Van Kauwenbergh forecast that the reserves will last for 300–400 years [5]. These conventional fertilizer production methods need to be fully or partially replaced by sustainable and environmentally friendly processes.

Wastewater is a potential source of nitrogen, phosphorous, and other nutrients that originate from human and industrial waste. Traditionally, the goal of wastewater treatment plants (WWTPs) is to remove these nutrients along with organic compounds, as their release into the environment can cause major problems such as eutrophication [6]. Removing of these compounds is costly. For instance, nitrogen is removed through the nitrification–denitrification process, which requires a large amount of energy for aeration. It has been estimated that the aeration energy demands are about 50–70 % of the total energy

* Corresponding author.

E-mail address: raed.al-juboori@aalto.fi (R.A. Al-Juboori).

<https://doi.org/10.1016/j.seppur.2022.122250>

Received 26 May 2022; Received in revised form 25 September 2022; Accepted 25 September 2022

Available online 27 September 2022

1383-5866/© 2022 The Author(s). Published by Elsevier B.V. This is an open access article under the CC BY-NC-ND license (<http://creativecommons.org/licenses/by-nc-nd/4.0/>).

Nomenclature	
A	Membrane fiber area (m^2)
A_f	Filter paper area (m^2)
a_w	Water activity (-)
B_w	Water vapor permeability through the membrane material
b	Slope of t/V versus V
c	Mass of solids deposited on filter paper (kg)
D_h	Hydraulic diameter (m)
$D_{NH_3,m}$	Ammonia diffusion coefficient in the membrane (m^2/s)
$D_{NH_3,w}$	Ammonia diffusion coefficient in water (m^2/s)
$d_{s,i}$	Inner diameter of membrane module (m)
$d_{f,o}$	Outer diameter of membrane fiber (m)
$d_{f,i}$	Inner diameter of membrane fiber (m)
J_w	Water vapor flux across the membrane ($kg/m^2.s$)
K	Overall mass transfer coefficient of ammonia (m/s)
K_l	Ammonia mass transfer coefficient on lumen side (m/s)
K_m	Ammonia mass transfer coefficient in membrane's pores (m/s)
K_s	Ammonia mass transfer coefficient on shell side (m/s)
n	Number of membrane fibers (-)
P	Vacuum pressure applied for sludge filterability test (Pa)
p_{ws}^0	Water vapor pressure on shell side (Pa)
p_{wl}^0	Water vapor pressure on lumen side (Pa)
Q	Ammonia water flow rate (m^3/s)
Re	Reynolds number
Sc	Schmidt number
Sh	Sherwood number
T	Temperature ($^{\circ}C$)
t	Filtration time for filterability test (Sec)
V	Volume of filtered sludge (m^3)
X_s	Molar fraction of solute
<i>Greek letters</i>	
α	A parameter of Equation (3) that depends on the type of solute
β	A parameter of Equation (3) that depends on the type of solute
γ	Concentration polarization coefficient (-)
ε	Membrane porosity (%)
μ	Water viscosity (kg/m.s)
ρ	Water density (kg/m^3)
τ	Membrane tortuosity (-)

requirements at WWTPs [7]. In addition, removal processes do not offer the opportunity to recover resources; rather, they convert them to other forms that have minimal impact on the environment. However, the conversion is not always efficient in obtaining the desired final products. The nitrification–denitrification process does not solely produce N_2 . Other gases of concern, such as N_2O and NO , are also released in this process [8]. N_2O is a worrying greenhouse gas. It has a long life of 121 years and a large cumulative 100 years with a global warming potential of 265. Similarly, P removal—whether through biological or chemical paths—requires intensive energy (e.g., carbon source and aeration) or the application of expensive chemicals (e.g., iron or aluminum salts) [9]. Thus, recovering nutrients from the wastewater stream not only helps relieve the pressure on conventional sources and processes for fertilizers, it also reduces energy requirements associated with nutrient removal.

There are several technology options for nutrient recovery, such as air stripping [10], membrane technologies (forward osmosis, membrane distillation, and reverse osmosis) [11–13], struvite crystallization [14], and membrane contactor [15]. Although air stripping is a mature technology with high nitrogen recovery efficiency, it requires high energy for aeration and heating, which may render the technology costly [2]. Similarly, membrane technologies require a high amount of energy for the high pressure or temperature required for operation. Despite the maturity and growing implementation of struvite crystallization worldwide, the required equimolar presence of Mg , PO_4^{3-} and NH_4^+ for struvite precipitation may limit the technology economic feasibility [16,17]. Membrane contactor technology, on the other hand, seems to offer an attractive solution for nitrogen recovery with low energy requirements, as it operates at atmospheric pressure and temperatures and does not require aeration [18].

Membrane contactor technology utilizes a hydrophobic membrane that serves as a barrier between the ammonia-rich liquid and the stripping solution (acids). The membrane allows released ammonia gas from liquid at an elevated pH (over 8.6) to diffuse through its pores to be absorbed on the other side by the stripping solution [6]. Most of the studies testing membrane contactors for nitrogen recovery use commercially available contactors that have a low tolerance to high solids concentrations, which is the case with wastewater streams. Additionally, nitrogen recovery with membrane contactors has primarily been conducted with synthetic samples or urine [2,19], which are both characterized by their low solids content. This study reports on

the field application of a novel pilot-scale membrane contactor system developed by Aalto University (referred to as NPHarvest) that can handle high solids concentration through augmenting the system with a coagulation/flocculation/precipitation step that helps in recovering phosphorus at the same time. This system was tested in our previous studies with different wastewater streams and proved its potency with nitrogen recovery and effective phosphorous removal [15].

The goal of this work was to evaluate the performance of the developed system for long-term trials applying different operating conditions and pre-treatment options. While previous studies tested operating conditions such as liquid bulk pH, hydraulic retention time, and stripping acids types and strengths, these tests were performed using lab-scale setups and a simple matrix feed solution under a controlled environment [2,20]. In this study, the system was fed straight from a mesophilic digester at the Viikinmäki WWTP in Finland, where a real-time variation in feed quality was experienced. This provides important insights into the tolerance of the membrane contactor technology in a typical real-life environment for this technology. Three bulk pH values of 9, 10, and 11 were tested along with three hydraulic retention times of 2 h, 4 h, and 8 h. The most commonly applied stripping solution for nitrogen recovery in membrane contactor systems is sulfuric acid. However, this study tested other common acids such as HNO_3 and H_3PO_4 . The motivation behind using these acids is to study NPHarvest performance with these acids. Additionally, these acids produce ammonium salts that have a higher content of N and P, and this could potentially increase the value of the end product. For the NPHarvest pre-treatment step, we normally apply poly aluminum chloride and polymer for coagulation-flocculation and induce the precipitation with lime kiln dust (LKD). In this work, we tested the application of starch as an alternative to inorganic coagulants and polymers. The effect of the above-mentioned parameters and pre-treatment options on ammonia recovery and phosphorus and solids removal was monitored using on-line and laboratory measurements. However, it should be noted that the purpose of this study was not to achieve steady state conditions of the system, but rather to examine the effect of the different parameters on the system performance. The obtained experimental data were analyzed theoretically to gain an understanding of the effect of different parameters on the mass transfer of ammonia in the process.

NPHarvest produces ammonium salt solutions and P-rich sludge. The quality of the NPHarvest products from hygienic and hazardous

chemicals contents was tested in our previous study and proven to be of a reasonable caliber [15]. It is worth mentioning that P concentration in the sludge depends on a number of factors such as the initial concentration in the waste stream, the concentration of solids in the stream and the used chemicals for P precipitation. For instance, P concentration in the sludge produced from urine is higher than that produced from reject water due to the high initial P concentration and low solids content in urine compared to reject water. In this work, we studied the physical and chemical properties of produced sludge by applying cake filterability measurements, sludge volume index (SVI), thermogravimetric analysis, and elemental and metals analyses. The purity and elemental content of the produced ammonium salts have also been investigated. A quality analysis of membrane contactor products has rarely been addressed in the literature, and their presentation and discussion in this study would help in constructing a comprehensive evaluation of the technical feasibility of nutrient recovery.

2. Materials and methods

2.1. Site and stream description

The Viikinmäki WWTP is the largest plant in Finland. It treats wastewater coming from around 900,000 inhabitants for an average of 100 million m³ per year. Around 85 % of the total wastewater is of domestic origin, and the rest comes from local industries. At this WWTP, an activated sludge process is used to treat wastewater. The treatment train at the Viikinmäki WWTP is composed of screening and grit removal, pre-aeration, a chemically enhanced primary sedimentation unit where settleable particles, colloids, and phosphorus are removed, an activated sludge process with advanced nitrogen removal and post-denitrifying filters, secondary sedimentation for collecting sludge produced from the nitrification-denitrification process, and a biological filter for further nitrogen removal. Phosphorus is removed through precipitation by adding ferrous sulfate in grit removal and at the end of the bioreactors [21].

The sludge produced from primary and secondary sedimentation tanks is collected in the anaerobic digestion (AD) tank in which the volume of sludge is reduced, and methane is generated for energy production. Digestate is the product of the AD process, and the liquid content is further reduced by dewatering using centrifuges. The liquid fraction generated from this last step is referred to as reject water—the wastewater used in this study. The characteristics of this water fraction are presented in Table 1. The minimum, maximum, and average values of the characteristics were provided by Viikinmäki WWTP operators during June–October 2018. These values are presented to illustrate the fluctuation in wastewater quality over time. The last column presents the average values of the characteristics along with their standard deviation for samples collected during January and February 2020 [22]. All the measurements were conducted in triplicate.

2.2. NPHarvest system – Description and process design

The NPHarvest system used in this work is shown in Fig. 1. As mentioned in the previous section, the reject stream coming from a mesophilic digester was fed to the system. The feed flow was controlled

by a ball valve that receives a signal from a leveling sensor in the feed tank. The feed tank is equipped with an NH₃-N probe (AN-ISE sc-anturi RFID, Hach) for the online measurement of ammonia levels in the reject water. The wastewater was then pumped to the pre-treatment unit, which consists of slow and fast mixing where phosphorous and solids were removed through coagulation/flocculation with Polyaluminum Chloride (PAX-XL 100) and a polymer (Superfloc A120) as one pre-treatment option and modified starch (PrimePHASE 3545) as another pre-treatment option. The PAX/polymer or starch dosage was set based on the outcomes of our earlier studies in developing the system [15,23]. The applied concentrations of PAX, polymer, and starch were 278 g/L, 0.1 g/L, and 3.5 mL/L, respectively. The respective flow rates applied for these chemicals were 0.66 L/h, 0.41 L/h, and 1.43 L/h. The coagulation/flocculation was conducted at an elevated pH range of ca. 9–11 to convert ammonium to ammonia gas for the subsequent nitrogen recovery step. The effect of the three bulk pH levels of approximately 9, 10, and 11 on nitrogen recovery was evaluated. Slaked lime provided by Nordkalk was used as an alkaline agent (30 g/L) to raise the pH of reject water. Slaked lime was selected over other alkaline agents such as NaOH, due to its low cost that improves the economic competitiveness of NPHarvest technology [15]. Additionally, lime is used at the Viikinmäki WWTP which makes it a readily accessible material for the recovery process. Although lime can increase sludge volume and consequently reduce P concentration in the sludge, the application of lime is justifiable for the case of reject water where P is already low (14 mg/L on average). Sludge with high concentration of calcium can be a useful soil amendment product for acidic soils even with small P content. The dosing of lime was controlled based on the measured pH level in the fast-mixing tank, which was measured through a pH meter that continuously logs data into the programmable logic controller (PLC) unit in the system. As the flocculated water left the slow mixing tank, LKD with a concentration of 15 g/L was added to the line to accelerate the settling of the formed flocs. Similar to PAX and polymer, the LKD dosing was pre-determined based on earlier observations of the system performance (flow rate = 6.8 L/h).

The formed sludge in the settling tank was pumped into a bag filter fixed on top of the feed tank. The frequency and flow rate of sludge discharge were set depending on the selected flow of the feed pump. The bag filter was used in this work as a practical and cost-efficient solution to collect and dry the sludge while the NPHarvest system is in operation. The bag was replaced when it was filled. The sludge line was redirected to the outlet stream of the system when the bag filter was not used. The supernatant in the settling tank was fed to the equalization tank gravimetrically. The equalization tank is equipped with a leveling sensor. When the liquid reaches a high level on the tank, the sensor sends a signal to the PLC to stop the feed pump to avoid overflow of the system. If the feed pump is turned off, the chemical pumps stop to avoid overdosing the system. The equalization basin is also equipped with a suspended solids (SS) probe (ATS430 - Aztec ATS430 Turbidity probe, ABB) to monitor the efficiency of the pre-treatment unit.

The pre-treated water in the equalization tank was pumped to the membrane contactor that contains six modules of multi ePTFE membrane tubes (modules detailed description and membrane characterizations are provided in our previous work [15,24]). The total number of fibers inside the contactor is 500. Each fiber has a length of 1 m and an internal diameter of 1 cm with wall thickness of 1 mm. The membrane fiber porosity range is 70–90 % with an internodal distance of 10–30 μm. The homogeneity of the liquid in the contactor tank was maintained using a parabolic mixer. While the treated reject water flowed through the membrane contactor tank, a selected acid type with a certain strength was pumped through the lumen side of the fibers. The acid flow rate was kept at 5 L/h per module throughout the whole test (collective acid flow through the six modules = 30 L/h). Three different acids were tested in this work: sulfuric, phosphoric, and nitric acid. The impact of the acid strength on nitrogen recovery was also gauged using sulfuric

Table 1
Viikinmäki reject water characteristics.

Constituents	Minimum (mg/L)	Maximum (mg/L)	Average (mg/L)	Measured in lab (mg/L)
TN	791	1072	909	1231 ± 7
TP	8	26	14	12.75 ± 0.13
SS	550	2225	1116	1100 ± 37
pH	7.9	8.1	8	8.1 ± 0.15
NH ₄ ⁺ -N	636	801	723	688 ± 11

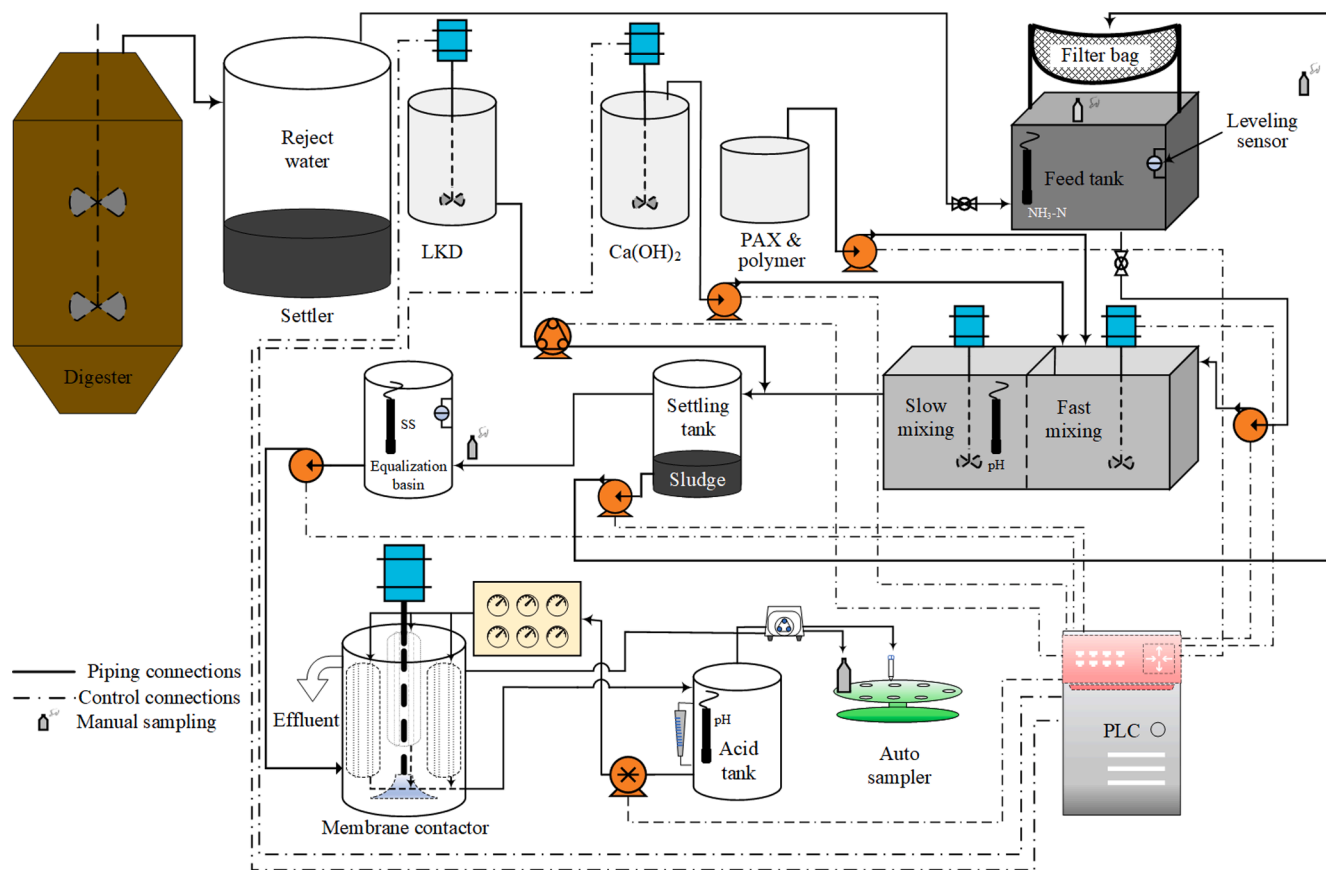


Fig. 1. Schematic of the NPHarvest system. The digester and the settler tank are not part of the system, and their scale does not reflect the true proportionality of their size in comparison to the system components.

acid with different concentrations of 0.5, 1, and 2 M.

The retention time of all the units except the membrane contactor is fixed throughout the piloting period. For the membrane contactor, three hydraulic retention times (HRTs) were tested: 2 h, 4 h, and 8 h. Most of the runs were conducted at a retention time of 8 h where the effects of bulk pH, acid type, and strength—and the pre-treatment options—were tested. The retention time of the membrane contactor was controlled by setting a fixed flow value for the feed pump. All tests were performed at a fixed speed for the membrane contactor mixer of 50 Hz, except for the last test, where the speed was lowered to 25 Hz. The online measurements of the different water characteristics were compared to the values obtained from a lab analysis of manually collected samples to verify the accuracy of the online measurements.

2.3. Schedule

The piloting schedule of this study is detailed in Table 2. Before starting the pilot tests, the membrane fibers were washed by filling the reactor with diluted acid for a day. The first three runs were conducted to select the most efficient HRT. A long HRT was selected for running most of the piloting trials to keep daily chemicals consumption as low as possible so the pilot does not run out of chemicals at times when it is not attended (e.g., nighttime). Sulfuric acid was selected as the preferred acid, and different acid strengths were tested to evaluate the change in the ammonia transfer rate. The acid was changed after each run.

2.4. Sampling and analysis

During the pilot test, the selected sampling points were as follows: influent tank, settling tank (sludge samples), equalization basin, membrane contactor, and acid tanks. Manual samples were collected from

Table 2
Test schedule at the Viikinmäki WWTP.

Run No.	Run purpose	Contactor mixer speed (Hz)	HRT (h)	Acid type	Bulk pH
1	HRT	50	8	1 M H ₂ SO ₄	11
2	HRT	50	4	1 M H ₂ SO ₄	11
3	HRT	50	2	1 M H ₂ SO ₄	11
4	Acid strength	50	8	2 M H ₂ SO ₄	11
5	Acid strength	50	8	0.5 M H ₂ SO ₄	11
6	Bulk pH	50	8	1 M H ₂ SO ₄	10
7	Bulk pH	50	8	1 M H ₂ SO ₄	9
8	Acid type	50	8	0.5 M H ₃ PO ₄	11
9	Acid type	50	8	0.5 M HNO ₃	11
10	Coagulant type —starch	50	8	1 M H ₂ SO ₄	9
11	Lower mixer speed	25	8	1 M H ₂ SO ₄	11

three locations: the feed tank, recirculating sludge line, and settler overflow. Samples from the membrane contactor tank and acid tank were collected using an in-house-built auto-sampler connected to a peristaltic pump. A Raspberry Pi 4 Model B was used to control the peristaltic pump and a stepper run by a Python program. The stepper was used to spin the sampler tray around, and the peristaltic pump was

connected with two tubes for withdrawing samples from the membrane contactor and acid tank at the same time. 0.5 L bottles and 10 mL tubes were used to collect membrane contactor effluent and acid samples, respectively. Samples from the membrane contactor and acid tank were collected automatically every 4 h throughout all the runs, while other samples were collected manually once a day.

The collected samples were analyzed for $\text{NH}_3\text{-N}$ (APHA 4500- $\text{NH}_3\text{ D}$: Ammonia-Selective Electrode Method) and SS (APHA 2540 D: Drying Method at 103–105 °C with the glass-fiber filter Whatman GF/A) [25]. Total phosphorous and orthophosphate were measured using the Blu-Vision Analyzer (Skalar, Netherlands) following the ascorbic acid method (4500-P E [26]) and SFS ISO 15923-1 standard, respectively. The products collected from NPHarvest (namely, ammonium salts and phosphorous rich (P-rich) sludge) were characterized. The nitrogen content of ammonium salts was determined using the CHNS/O Elemental Analyzer (Thermo Scientific, FlashSmart EA). Sulfanilamide was used as the standard for elemental analysis. The metal content of ammonium salts and P-rich sludge samples was measured using X-ray fluorescence (XRF) (Malvern Panalytical, Axios mAX 3 kW). About four grams of samples were used for the XRF analysis. The physical characteristics of the collected sludge samples were also analyzed by measuring the Sludge Volume Index (SVI_{30}), filterability, and cake resistance, following the methods detailed in [27]. The thermal properties of dried sludge samples were studied using Thermogravimetric–Mass spectrometric (TG-MS) analysis. These measurements were performed using the thermal analyzer, NETZSCH STA 449 F3 Jupiter, equipped with the mass spectrometer model QMS 403 Aeolus Quadro for gas analysis. The details of the TG-MS measurements are available in [27].

3. Results and discussions

3.1. Effect of treatment conditions on suspended solids

The variation in SS concentrations for settling and equalization tanks as well as the effluent of the membrane contactor are depicted in Fig. 2. The average of the SS in the equalization tank is also presented as a solid line. The average of each run was calculated by dividing the sum of the solids for each run by the number of data points. The SS data for the

equalization tank were captured using the online system for data acquisition, while the data points of the settler and the membrane contactor were obtained through sampling and laboratory measurements.

It can be seen that the SS concentration measured from the settling overflow was higher than that of the equalization tank in some instances and on par with it in other instances. This could be attributed to the timing of the manual sampling collection. If the sampling coincided with times where the sludge withdrawal was on, this could agitate some flocs, which may increase the SS in the collected samples. The high SS concentration in the settler overflow is also related to the treatment efficiency. When the bulk pH was lowered to 9, the solids increased significantly indicating poor floc formation. Similarly, when there was a malfunction in the LKD dosing in the starch trail, light flocs developed. This suggests that optimization of settling process is required for the different pre-treatment conditions. The high SS in samples collected from the settler compared to that of the equalization tank suggests that settling took place in the equalization tank. Indeed, we observed a layer of solids precipitated in the tank after the completion of the pilot testing. The SS concentration of the membrane contactor effluent was lower than that of the equalization tank throughout most of the piloting period. This decrease is most likely due to solids deposition onto surfaces in the membrane contactor. This can result in membrane fouling which could impact ammonia recovery. However, since the process is not pressurized, solids adhesion onto membrane surface is expected to be loose. Based on our experience with NPHarvest system, fouling formation on membrane surface did not significantly impact NH_3 recovery for operation time of up to two months. We recommend cleaning with diluted acids as a maintenance routine after operation with such a period. Fouling formation and cleaning of PTFE fibers was studied on small and pilot scales in our previous studies [15,24].

When scrutinizing the effect of the different testing conditions on SS concentration, one can notice that retention time (in other words, the flow rate) did not have an explicit effect on the SS concentration in the treated water, as the level was fluctuating between around 350 mg/L and 700 mg/L. However, bulk pH seems to have a clear effect on SS concentration. A bulk pH of 10 appears to be the best pH level, where SS concentrations varied between a maximum of approximately 450 mg/L and a minimum of approximately 300 mg/L. Lowering the pH to 9

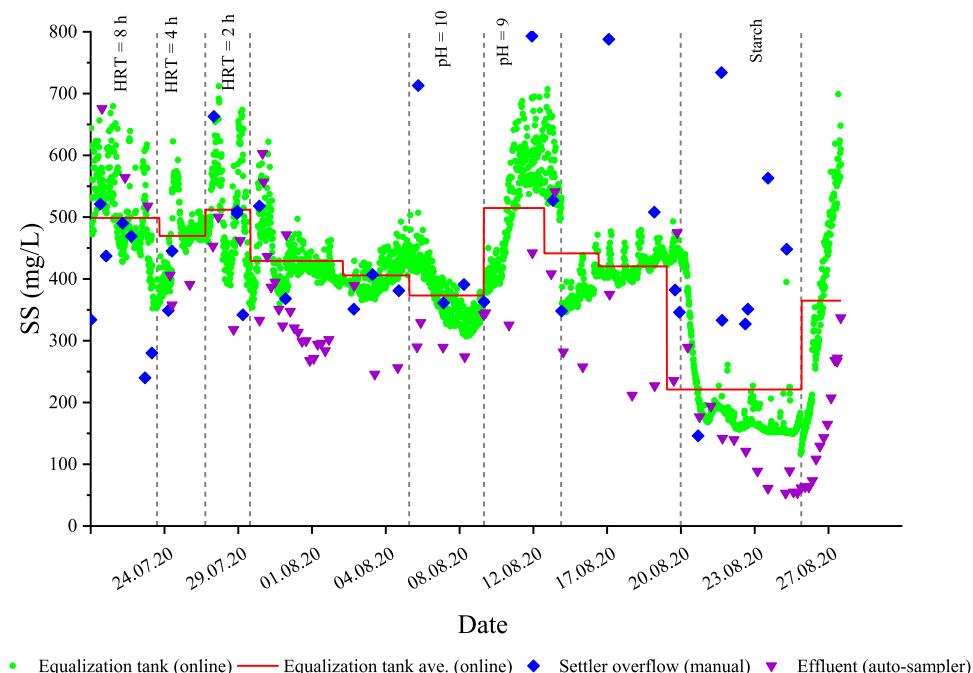


Fig. 2. SS concentration profile post pre-treatment stage.

gradually increased the SS to a maximum of 700 mg/L. Increasing the bulk pH to 11 could also increase the SS to approximately 700 mg/L but rather in a fluctuating manner. The increase in SS concentration in the treated water in the equalization tank can be explained by three scenarios: the inefficient removal of SS, the excess from the $\text{Ca}(\text{OH})_2$ dose applied to raise the pH, and the fluctuation in the influent SS level. The SS level in the influent was manually measured daily (Fig. 3) to interrogate its effect on removal efficiency. The results (presented in Figs. 2 and 3) suggest that the SS increase at pH 9 is mainly due to low SS removal efficiency at this pH level as there was no abnormal spike in the influent SS (470–670 mg/L). The high SS concentration at pH 11 can be attributed to both the elevated levels of $\text{Ca}(\text{OH})_2$ applied and the high SS received in the influent in some instances, especially at the start (SS up to ~880 mg/L).

When comparing SS removal with the PAX and Superfloc A120 treatment with that of starch, it can clearly be seen that the latter achieved better results. The average SS concentration in the first case was around 440 mg/l, while in the second case, it was around 170 mg/l. This is translated into average SS removals of 30 % and 73 % for PAX + Superfloc A120 and starch, respectively.

3.2. Effect of treatment conditions on ammonia concentration and recovery efficiency

Ammonia concentrations of influent, settler overflow, and effluent are depicted in Fig. 4 with dividing lines that highlight the runs where different treatment conditions were applied. Interestingly, the ammonia concentration in the settler overflow was higher than that of the influent. Considering that the pre-treatment does not add any ammonia to the wastewater, the high level of ammonia in the settler can be explained by the accumulation that occurs due to the high retention time in the settler caused by feed pump stoppages for controlling the retention time in the membrane contactor unit. The other plausible explanation for the elevated ammonia levels in the settling tank is the release of ammonia from the sludge blanket. Based on this, nitrogen recovery efficiency was calculated in two ways—for the membrane contactor and for the overall system, as shown in Fig. 5. The former takes into account the ammonia concentration drop between the settler overflow and the effluent, while the latter was calculated based on the ammonia concentration variation between the influent and effluent. The efficiency calculations for both cases were performed using the average values of

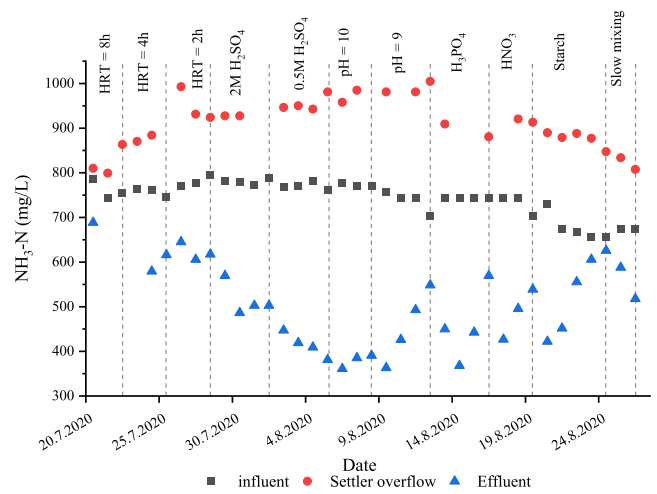


Fig. 4. Ammonia concentration profile for influent, overflow settler, and effluent lines throughout all runs.

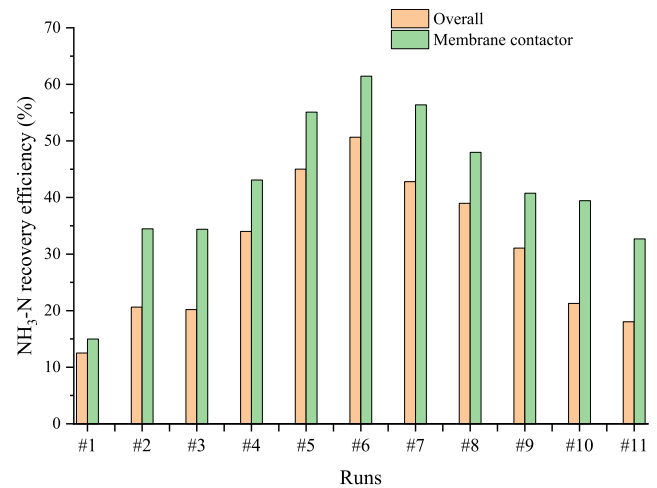


Fig. 5. $\text{NH}_3\text{-N}$ recovery efficiency for piloting runs.

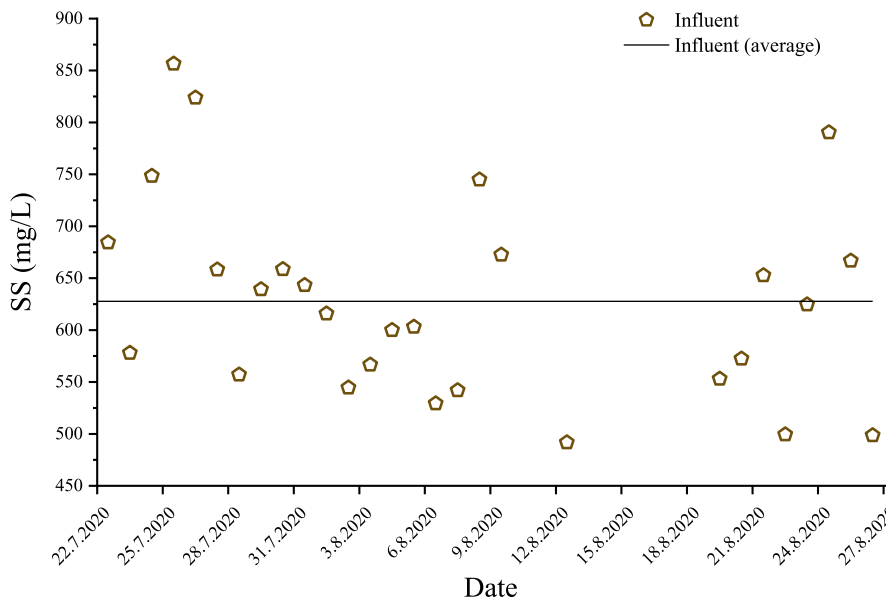


Fig. 3. SS concentration of influent.

NH₃ for each run. It is noteworthy that ammonia losses into the atmosphere due to inevitable imperfections in the system concealment (such as openings for the mixers' shafts) have not been taken into account in this study. However, scrutinizing the ammonia mass balance and identifying hotspots for ammonia losses in the system are planned for our upcoming research work.

The first three runs were designated to test the effect of hydraulic retention time on nitrogen recovery. The data from the first run were a bit distorted, especially for ammonia levels in the settler and membrane contactor tanks due to system instability during the start-up phase. Thus, it is hard to make a fair judgment based on the data collected from the first run. The second and third runs show that decreasing the HRT from 4 h to 2 h (corresponding to an increasing feed flow from 2 L/s to 4 L/s) had an insignificant effect on nitrogen recovery, as shown in Fig. 5. The results for runs 4 and 5 reveal that applying 0.5 M H₂SO₄ resulted in better ammonia recovery than when applying 2 M. This is likely due to the effect of viscosity and water vapor transfer across the membrane. The effect of varying the acid concentration in the stripping solution (H₂SO₄) from 5 % to 10 % was found to increase the absorption efficiency by only 0.002 % [28]. Considering the acid concentrations tested in this study (0.5 M and 2 M), these concentrations correspond to volume percentages of ~3–11 %, suggesting that the effect of viscosity alone cannot explain the drop in nitrogen recovery efficiency. Water vapor transport across a hydrophobic membrane is driven by the difference in the water vapor pressure (p^0) and activity (a_w) between the shell side and lumen side, as shown in Equation (1) [29]. Based on the Antoine equation, water vapor pressure depends on the temperature of the water (Equation (2)) [30]. The water temperature in the membrane contactor tank is almost the same as that in the acid tank, hence the water vapor transport is only affected by water activity differences across the membrane. Water activity can be calculated by applying Equation (3) [31]. It is clear from this equation that increasing the acid concentration reduces water activity on the lumen side, which in turn increases the water activity difference, consequently leading to more water vapor transfer across the membrane. The water vapor competes with ammonia and negatively impacts its stripping efficiency. The effect of activity seems to be a more plausible explanation for the drop in ammonia recovery when the acid concentration was increased. When calculating the water activity on the lumen side for 0.5 M and 2 M H₂SO₄—applying Equation (3) and using the same values for α and β as those reported in [19]—it was found that such an increase in acid concentration results in a water activity drop from 0.9911 to 0.9667. This was evident in the higher increase in the acid tank level of 2 M (25 cm) compared to that of 0.5 M (20 cm). It should be noted though that membrane wettability was negligible throughout the testing of NPHarvest with this streams and other waste stream. The measurement of contact angle of the fouled fibers in our previous study showed insignificant loss of the angle of less than one degree [15]. The effect of acid concentration on the ammonia accumulation rate in the acid will be discussed in later sections.

$$J_w = B_w (p_{ws}^0 a_{ws} - p_{wl}^0 a_{wl}) \quad (1)$$

$$p_w^0(T) = e^{\left(23.1964 - \frac{3816.44}{T - 46.13}\right)} \quad (2)$$

$$a_w = (1 - X_s) \exp(\alpha X_s^2 + \beta X_s^3) \quad (3)$$

The effect of bulk pH on ammonia recovery efficiency is represented by the results of runs 6 and 7, which show that a bulk pH of 10 had the best recovery efficiency (overall efficiency of 50 % and membrane contactor efficiency of 60 %). When examining the Run 7 segment in Fig. 4, one can notice that the ammonia effluent concentration was sharply increasing as we lowered the treated water's pH. This indicates that the bulk pH of 9 may have resulted in lower ammonia recovery efficiency had the run lasted for a longer time. The high recovery

efficiency at pH 10 could be explained by the high SS removal at this pH. SS removal drops at a pH of 9. However, raising the pH to 11 using an excessive amount of lime can introduce more solids to the system. Some studies reported similar results with the same pH points investigated here, where a pH of 10 was found to have the best recovery efficiency and the highest economic feasibility on lab and pilot scales [6,32,33].

When comparing the ammonia concentration profile and recovery efficiency of runs 8 (0.5 M H₃PO₄) and 9 (0.5 M HNO₃) with that of Run 5 (0.5 M H₂SO₄), it is obvious that sulfuric acid had the best results, followed by phosphoric acid and then nitric acid. The differences in the performance of the tested acids are related to the availability of ammonia scavenging ions (i.e., PO₄³⁻, NO₃⁻, and SO₄²⁻) at different pH levels. This will be discussed in more detail in the following sections.

The use of starch for the first time on a pilot scale (Run 10) proved to be an effective alternative for PAX and polymer pre-treatment. The ammonia recovery efficiency of starch was better than those of runs 2 and 3, where similar pH and acid conditions were applied with various HRTs. The increase in ammonia effluent for the Run 10 segment after halfway could be due to the observed malfunction of LKD dosing that led to the formation of light flocs, which may have abstracted the ammonia transfer. This also shows up in the SS results in Fig. 2. The decreasing ammonia trend for the settler overflow and the increasing trend for the effluent suggest that there is the possibility of ammonia release from the light flocs in the equalization tank and membrane contactor.

The last run was conducted to test the effect of the membrane contactor mixer speed on ammonia recovery. The results of this run showed that lowering the mixer speed by half did not affect ammonia recovery. The recovery efficiency was slightly lower than those for runs with similar conditions (runs 2–3). This indicates that there is room for cutting down on some energy usage in the system, which can improve the competitiveness of NPHarvest with other developed technologies for nitrogen recovery.

The high ammonia concentration in the effluent is worth discussing here. Although various studies reported high ammonia recovery efficiency of close to 100 %, it is important to note that these studies either used synthetic solution [34], energy intensive pre-treatment filtration [35] or low solid waste stream (e.g. urine)[2]. The relatively low ammonia removal is an acceptable tradeoff for the cost-effectiveness and technical simplicity NPHarvest offers. Reaching high ammonia removal with NPHarvest is also possible through optimizing mixing regime, fiber packing density and membrane materials modification. Multi-stage contactor can also be implemented for high ammonia removal efficiency as it is the case in [35].

3.3. Ammonia transfer rate with different treatment conditions

The mass transfer coefficient across the membrane for performed runs was calculated applying Equation (4) [20]. The results are revealed in Fig. 6.

$$K = \frac{Q}{A} \ln \frac{[NH_3]_{inf}}{[NH_3]_{eff}} \quad (4)$$

It can be seen that reducing HRT significantly increased the mass transfer coefficient. Reducing HRT from 4 h to 2 h increased K about threefold. This is attributed to the reduced effect of concentration polarization on mass transfer across the membrane with an increased flow rate. It is also important to note that higher flow rates were more stable than lower ones. Reducing acid concentration improved mass transfer across the membrane, represented by an increase in K by 30 % when using a weaker H₂SO₄ concentration of 0.5 M than with 2 M. This was explained earlier as high acid concentration promoting more water vapor transfer across the membrane and hindering NH₃ passage through the fibers' pores. Among the applied levels of bulk pH, the highest mass transfer coefficient achieved was with a pH of 10, which is due to efficient solids removal at this pH. As for acid types, H₂SO₄ had the highest

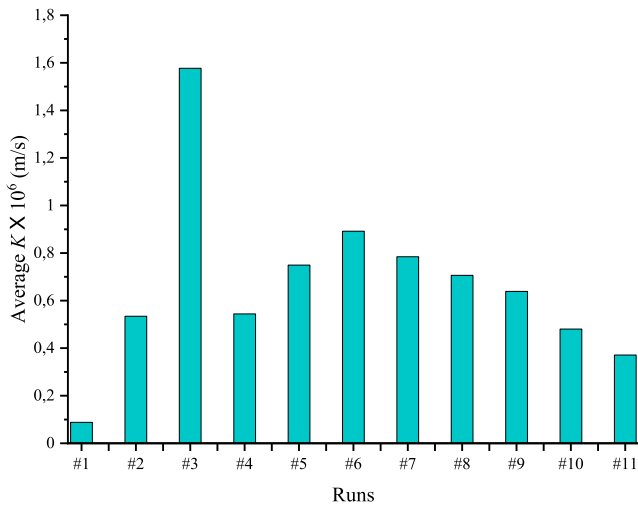


Fig. 6. Overall mass transfer coefficient for the conducted pilot runs.

mass transfer coefficient, followed by H_3PO_4 and then HNO_3 . A laboratory-scale investigation of nitrogen recovery from synthetic urine solution showed that HNO_3 and H_2SO_4 have the same ammonia transfer rate, which was higher than that of H_3PO_4 [2]. We believe that the outcome of our study is different from Damtie's study because their study was done for a short time (only 120 min), while ours was conducted for 3 days for each acid. The binding between nitric acid with ammonia tends to be quicker than the other two acids, and this means that mass transfer can be fast at the start of the run and then slows down for the rest of the period. This will be addressed in the following section, where the ammonia accumulation rate in the acid will be discussed in detail. The pre-treatment with starch (Run 10) had a comparable mass transfer coefficient to those done with PAX and polymer runs 2 and 3. Halving the contactor mixer speed slightly decreased the mass transfer rate of NH_3 across the membrane.

4. Effect of treatment conditions on ammonia accumulation rate

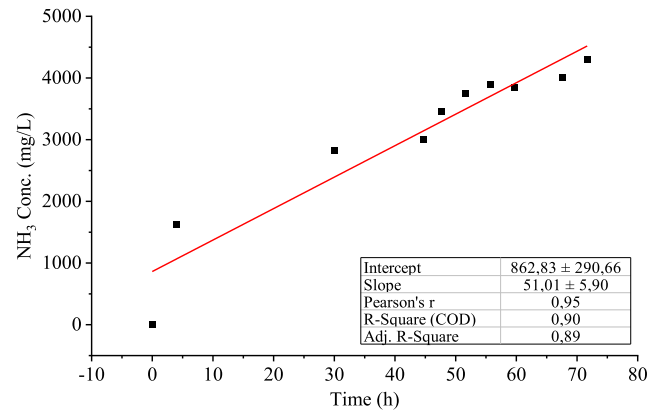
4.1. Hydraulic retention time (HRT) effect

The effect of the tested HRTs on the ammonia accumulation rate in acid is illustrated in Fig. 7. The accumulated ammonia was measured over a three-day period for each HRT. The ammonia accumulation rate expressed by $mg/L.h$ was quantified by taking the slope of the linear fitting of ammonia data over time, as shown in Fig. 7. Shortening the HRT clearly increases the ammonia accumulation rate. As we reduced the HRT from 4 h to 2 h, the accumulation rate increased to 112.8 $mg/L.h$ and 188.8 $mg/L.h$, respectively. This corresponds to a respective accumulation rate increase of 120 % and 270 % for an HRT of 4 h and 2 h compared to 8 h.

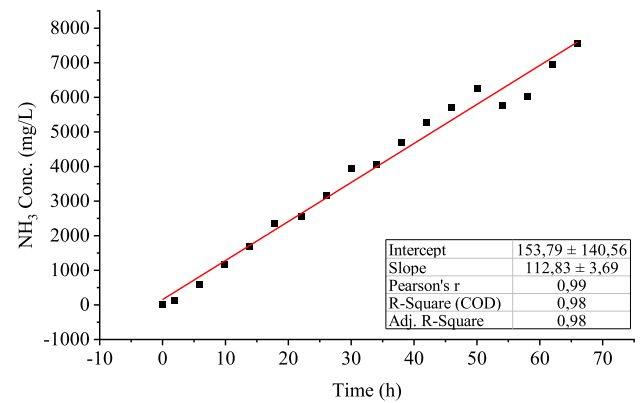
The improvement in the ammonia accumulation rate with decreasing HRT can be attributed to the positive effect of higher flows on mass transfer on the shell side and the reduction in concentration polarization. The impact of the water flow rate on the mass transfer coefficient on the shell side was evaluated by applying the Sherwood number formula, as presented in Equation (5) [20]. There are a large number of formulas for calculating the Sherwood number in the literature. The one selected in this study was quoted from Shen et al.'s work [36], as this formula was found to be adequately accurate for predicting the shell side mass transfer coefficient for commercial and handmade membrane contactor modules.

$$Sh = \frac{K_s D_h}{D_{NH_3, w}} = 0.055 \Re^{0.72} Sc^{0.33} \quad (5)$$

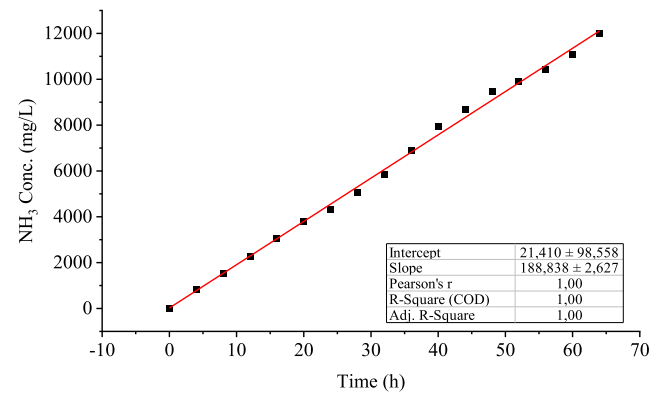
D_h and Re were calculated using equations (6) and (7) [36]:



(a)



(b)



(c)

Fig. 7. Ammonia accumulation rate in acid for different HRTs: (a) 8 h, (b) 4 h, and (c) 2 h.

$$\Re = \frac{4\rho Q}{n\pi\mu d_{f,o}} \quad (6)$$

$$D_h = \frac{d_{s,i}^2 - n d_{f,o}^2}{n d_{f,o}} \quad (7)$$

The value of the ammonia diffusion coefficient in water ($D_{NH_3, w}$) of $1.76 \times 10^{-9} m^2/s$ was adopted from [20] for performing the calculations of this study. The obtained K_s values of the three applied HRTs are shown in Table 3. It can be seen that reducing HRT from 4 h to 2 h increased K_s by about 65 %.

The effect of HRT on concentration polarization was evaluated by calculating the concentration polarization coefficient (γ) using Equation

Table 3
 K_s and γ values for the tested HRTs.

HRT (h)	K_s (m/s)	γ (-)
8	3.44×10^{-7}	8.59×10^{-7}
4	5.66×10^{-7}	8.65×10^{-7}
2	9.33×10^{-7}	8.68×10^{-7}

(8) [37]. The higher the value of γ , the lower the resistance to mass transfer. It is noteworthy that Equation (8) also accounts for resistance emanated from concentration polarization on the lumen side of the fibers. A fixed acid flow was applied in this study; thus the effect of resistance from the lumen side is the same for all the tested HRTs. The mass transfer coefficient on the lumen side denoted as K_l was calculated using the Sh formula reported in [20] (Equation (9)). The mass transfer coefficient of the membrane (K_m) is also the same for all HRTs. K_m was calculated using Equation (10) [20]. The diffusion coefficient of ammonia in membrane pores ($D_{NH_3,m}$) reported by Zhang et al. (2020) was applied in this study. The tortuosity of the membrane (τ) was calculated according to Equation (11) using a porosity of 80 % [38]. The calculated values of γ are presented in Table 4. It can be seen that reducing HRT resulted in a small increase in the concentration polarization coefficient, indicating a reduction in resistance to mass transfer across the membrane.

$$\gamma = \frac{K_s K_l}{K_s K_l + K_s K_m + K_l K_m} \quad (8)$$

$$Sh = \frac{K_l d_{f,i}}{D_{NH_3,w}} = 1.62 \quad (9)$$

$$K_m = \frac{\varepsilon D_{NH_3,m}}{\tau \delta} \quad (10)$$

$$\tau = \frac{(2 - \varepsilon)^2}{\varepsilon} \quad (11)$$

4.2. Acid concentration effect

The impact of stripping acid concentration on the ammonia accumulation rate was tested. The results are shown in Fig. 8. The lower the concentration of acid, the higher the accumulation rate. As discussed earlier, this observation is likely to be associated with the effect of acid concentration on water vapor transport across the membrane and acid solution viscosity. However, a concentration of 1 M exhibited a lower accumulation rate than 2 M. This was explained earlier as the run for 1 M H_2SO_4 was the first run, and the low ammonia recovery was ascribed to system instability rather than the effect of the acid concentration. The conversion of ammonia gas to ammonium ion on the lumen side depends on the availability of hydrogen ions. The hydrogen ion concentration for the tested acid concentrations was calculated, and the results were plotted against time (Fig. S.1). Less than half of the available hydrogen ions were consumed in producing ammonium sulfate with concentrations of 1 and 2 M. However, for the concentration of 0.5 M, almost all of the hydrogen ions available were consumed. This is expected as more concentrated acid requires more time to get all the available anions to bind to ammonia.

From the results presented in Fig. 8 and Fig. S.1, one can gather that

Table 4
 Sludge physical characteristics.

Treatments	SVI ₃₀ (mL/g)	$r \times 10^7$ (m/kg)
PAX/polymer (pH = 9)	18.93	15
PAX/polymer (pH = 10)	26.62	4.40
PAX/polymer (pH = 11)	29.72	4.20
Starch (pH = 9)	12.21	0.75

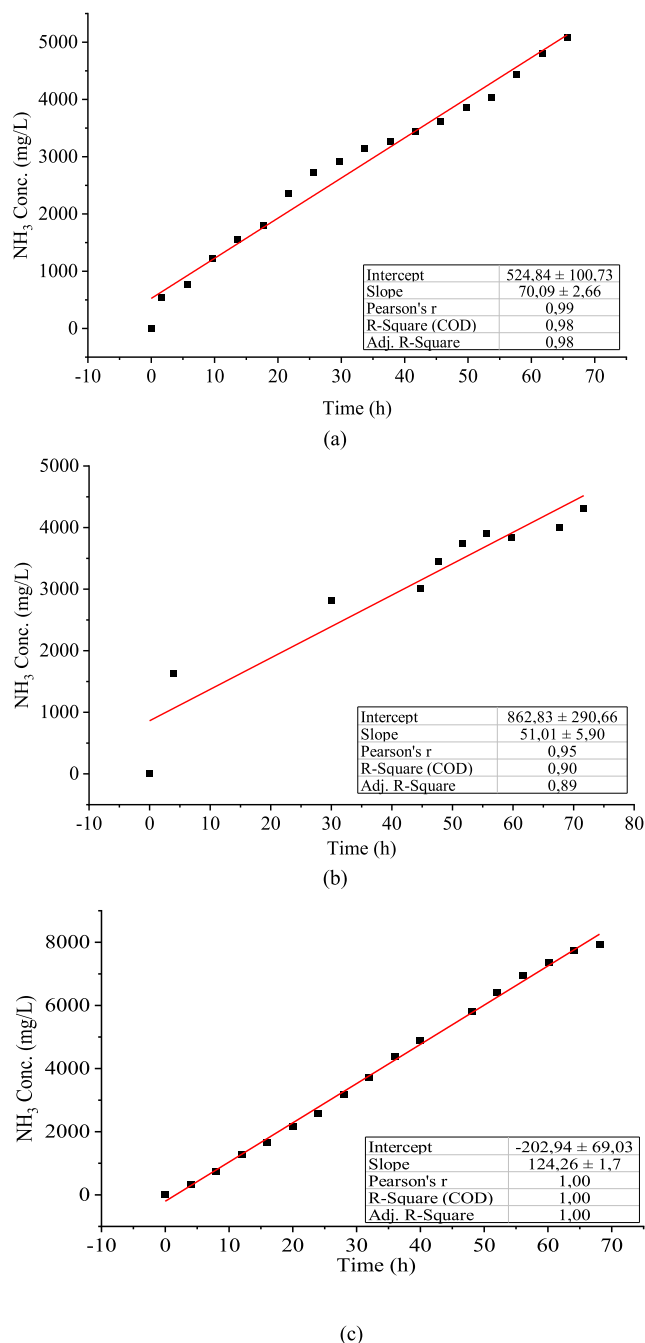


Fig. 8. Ammonia accumulation rate in acid for different H_2SO_4 concentrations: (a) 2 M, (b) 1 M, and (c) 0.5 M.

if the goal of the treatment is nitrogen removal, then the use of low concentrated acids is more feasible than the concentrated ones. Additionally, using low concentrated acids can be more economically viable and has less risk of degrading membrane materials over time. However, if the goal is recovering nitrogen and producing ammonium salts, then the use of concentrated acids is more sensible, as the accumulated amount of ammonia in the solution would be higher. The transport of concentrated ammonium solutions is more cost-effective than diluted solutions, and they require less energy to convert to crystalline salt. The goal of these experiments was not to reach acid exhaustion or a steady state, but rather to test the effect of acid concentration on nitrogen recovery.

4.3. Bulk pH effect

The pH of wastewater entering the membrane reactor is an essential parameter since in alkaline pH (>9), the ammonia/ammonium equilibrium presented in Equation (12) is shifted toward gaseous ammonia. The gas-permeable membrane inside the reactor allows gaseous ammonia to pass through and get absorbed by the extraction solution (acid).



The effect of bulk pH on the ammonia accumulation rate in the acid is illustrated in Fig. 9. Intuitively, increasing the pH increases ammonium conversion to ammonia, and ideally, it should result in an increase in ammonia accumulation in acid. At pH 10, most of the ammonium is

converted to ammonia, and a further increase in pH can only increase ammonia slightly. However, based on our observation, this was valid for increasing the pH from 9 to 10, but a further increase to pH 11 resulted in a decrease in the ammonia accumulation rate. This may be partly explained by the system instability during the first run of the pilot test, which coincides with a bulk pH of 11. When scrutinizing the results of other measurements, it can be noticed that increasing the bulk pH to 11 led to an increase in solids in the treated water (Fig. 2). The increase in solids can be due to the increased dose of slacked lime, or the drop in the removal efficiency of solids. A high concentration of solids in the bulk can negatively affect ammonia transfer across the membrane through different pathways. High solids can produce low shear forces in the boundary layer and promote membrane fouling [39]. A high concentration of solids could also hinder the mass transfer of volatile species [40]. It was also observed that suspended solids surfaces could capture ammonia, leading to a drop in ammonia recovery efficiency [41]. Increasing pH from 10 to 11 could significantly increase the conversion of ammonium to ammonia, and this comes with an increase in ammonia losses to the atmosphere. From these results, it appears that the bulk pH of 10 strikes a good balance between solids removal and ammonia losses, resulting in the best ammonia accumulation rate.

4.4. Acid type effect

The ammonium accumulation rate in sulfuric, phosphoric, and nitric acids over time is depicted in Fig. 10 a, b, and c, respectively. If considering only the ammonia concentration in HNO₃ before reaching a plateau (insert of Fig. 10c), then HNO₃ and H₂SO₄ had almost the same accumulation rate, while H₃PO₄ had a lower accumulation rate than these two acids. The plateau observed in the graph is an indication of the full occupation of all acid-active sites that bind with NH₃. These results agree with the findings reported in [2]. In their study, it was reported that sulfuric acid and nitric acid showed almost the same ammonia concentration after 1 h, while the ammonia concentration in phosphoric acid was lower.

Salt formation is related to hydrogen ion availability indicated by the pH level of the extraction solution (acid). Equations (13), 14, and 15 show the possible reactions between acids and their active species with ammonia at different pH levels [2]. Depending on the pH level of the acid solution, H₂SO₄ and H₃PO₄ could take up one or two ammonia molecules. Due to the importance of pH on the ammonia binding reaction, the pH of the tested acid solutions was recorded during the runs. The results are presented in Fig. S.2. Fig. S.2c shows that the pH change in HNO₃ is sharp compared to H₂SO₄ and H₃PO₄. This is related to the dissociation of the three acids and the produced protons and conjugated bases at different pH levels. HNO₃ has the highest dissociation constant ($pK_a = -1.30$), followed by H₂SO₄ ($pK_{a1} = -3$, $pK_{a2} = 1.92$), while H₃PO₄ has the lowest dissociation constant ($pK_{a1} = 2.15$, $pK_{a2} = 2.94$, $pK_a = 12.38$) [42]. At the starting pH of 1, H₃PO₄ is poorly dissociated. At pH 2, about 50 % of H₃PO₄ is dissociated to H₂PO₄⁻ and H⁺ (see Fig. S.3). The case is different for H₂SO₄ and HNO₃ as these acids are already dissociated at the starting pH of 1. At pH 2, the dissociation products of H₂SO₄ are 50 % HSO₄⁻ (scavenging 1 molecule of NH₃) and 50 % SO₄²⁻ (scavenging 2 molecules of NH₃). Although equations (13) and (14) show that elevated pH levels result in higher ammonia absorption, pH levels should not exceed 7 to avoid ammonia loss from the acid tank to the atmosphere. This limits the application of H₃PO₄, as the dissociation of the acid to active scavenging species such as HPO₄²⁻ can only start at pH > 5. However, the produced salt with H₃PO₄ has a higher value than salts produced with H₂SO₄, as the product contains both nutrients P and N. These findings suggest that to achieve the highest ammonia recovery possible, an automated acid changing/replenishing system based on pH level in the acid tank needs to be integrated into the NPHarvest system. To make an appropriate choice for acid type, several factors should be considered, such as the value and application of the end product, the effect of acids on construction

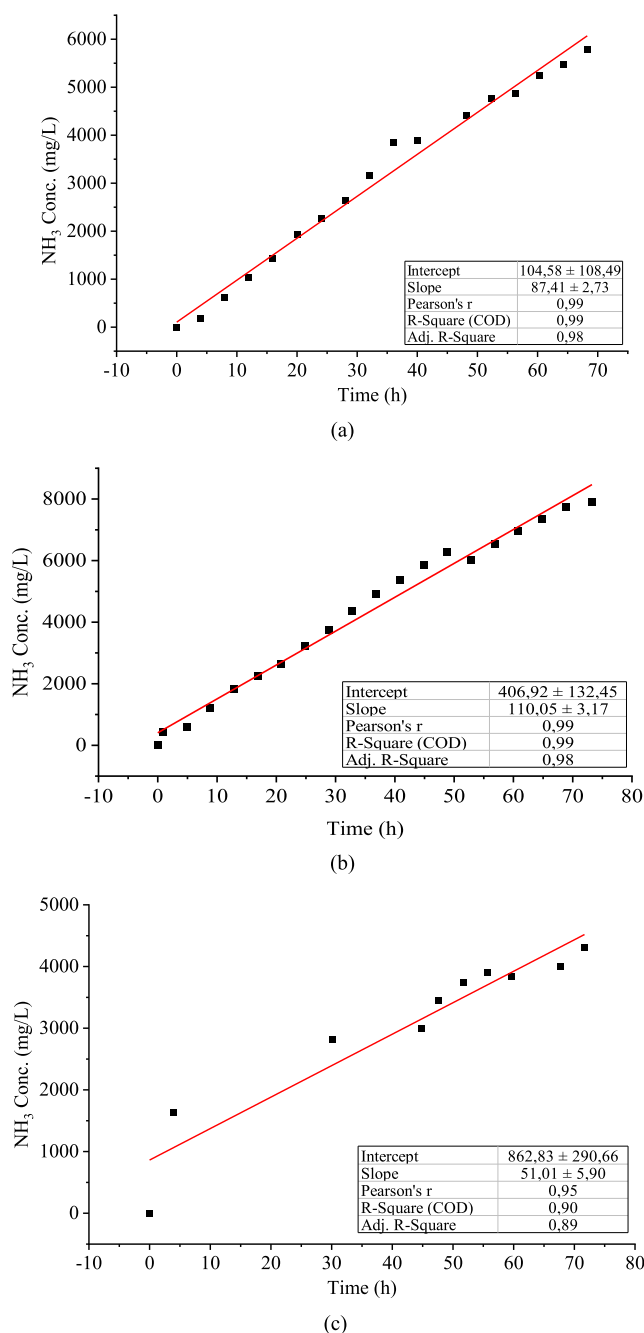


Fig. 9. Ammonia accumulation rate in acid for different bulk pH: (a) 9, (b) 10, and (c) 11.

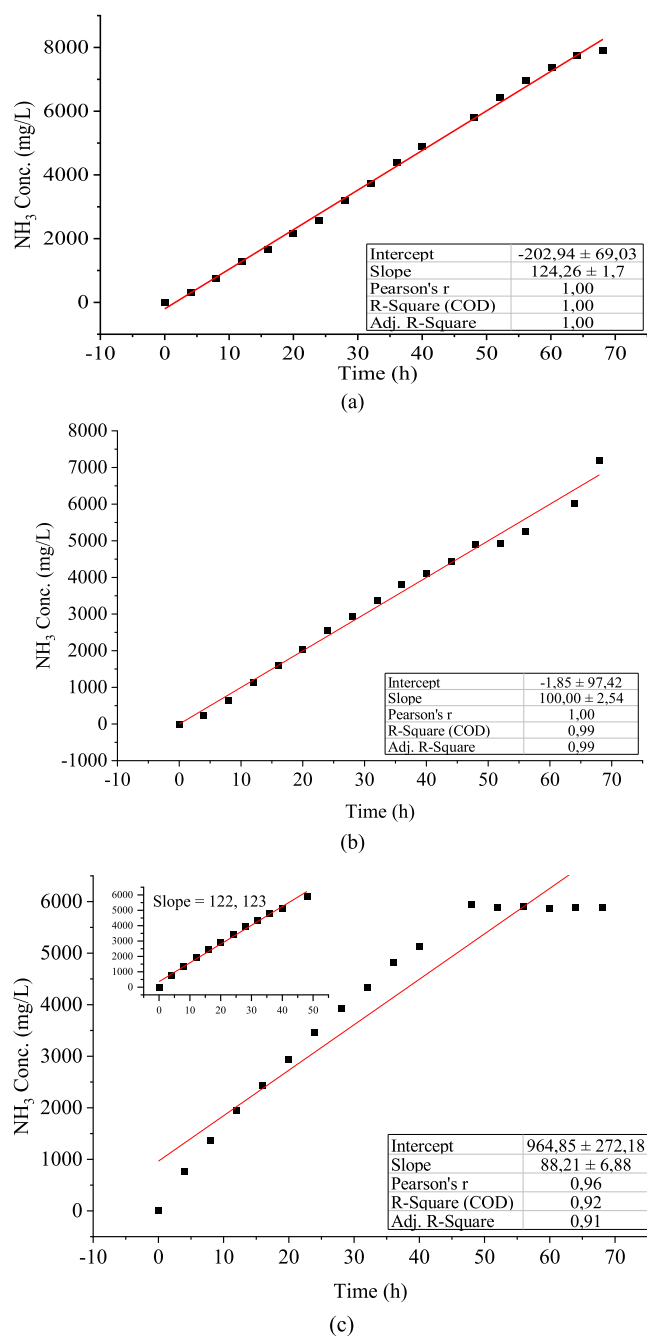
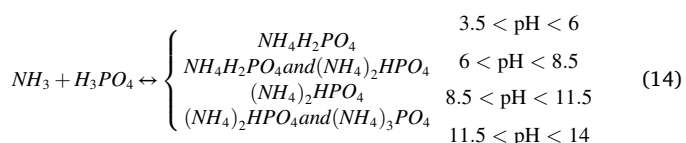
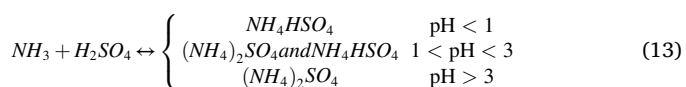


Fig. 10. Ammonia accumulation rate in acid for different acids with a concentration of 0.5 M: (a) H₂SO₄, (b) H₃PO₄, and (c) HNO₃.

materials of the system, and safe handling and storage of the product. For instance, ammonium nitrate is explosive, and this may require special precautions in dealing with the produced solutions or crystalline salt.



4.5. Effect of pre-treatment

The use of a commercially available starch-based product in the Finnish market known as PrimePHASE 3545 was explored as an alternative for conventional PAX and polymer pre-treatment. The ammonia accumulation rate for both pre-treatment options was recorded (Fig. 11). All of the test runs were conducted for three days, except for starch trials where runs went on for six days. Therefore, the ammonia accumulation rate represented by the slope of the linear fit was constructed for three days (insert of Fig. 11b) and for the whole period. It appears that for the first three days, starch had a sharp accumulation rate similar to that of PAX and polymer, and after that, the rate dropped. This is believed to be due to the glitch that occurred in the LKD feeding unit, which led to the formation of light flocs that are hard to settle and escape to the membrane contactor. There is a possibility of ammonia release from the loosely bonded ammonium with starch flocs or from the amine group existing in the starch structure [27]. These results align well with the data presented in Fig. 4, where an increase in ammonia effluent concentration was observed after the third day of operation with starch and LKD.

4.6. Effect of treatment conditions on phosphorous removal

Total phosphorous (TP) and orthophosphate concentrations and removal percentages for runs where bulk conditions were changed (pH, HRT, and pre-treatment options) are depicted in Fig. 12. As explained in the Methods section, the HRT of the membrane contactor was controlled by varying the feed flow to the system. This, in turn, affects the retention

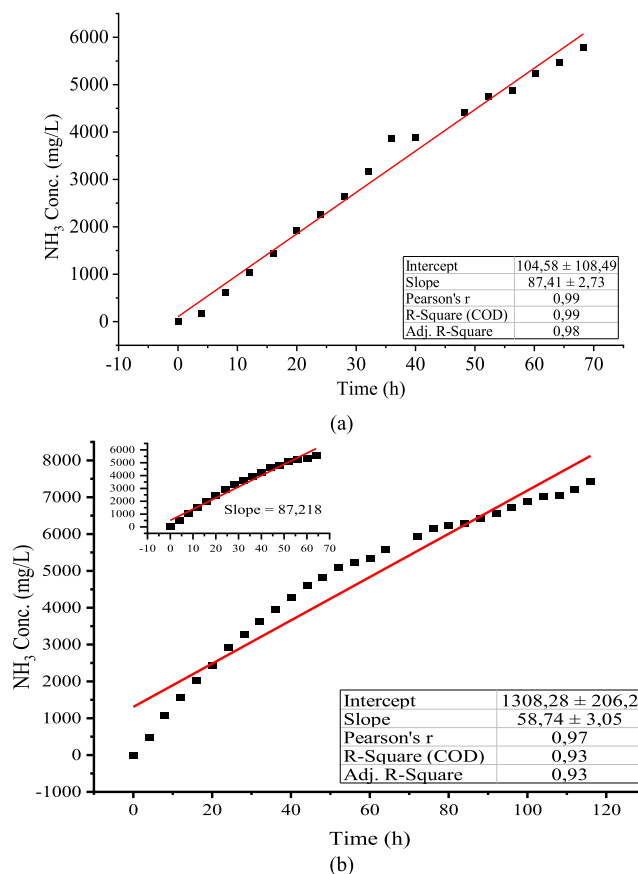


Fig. 11. Comparison between ammonia accumulation for (a) PAX and polymer treatment and (b) starch treatment.

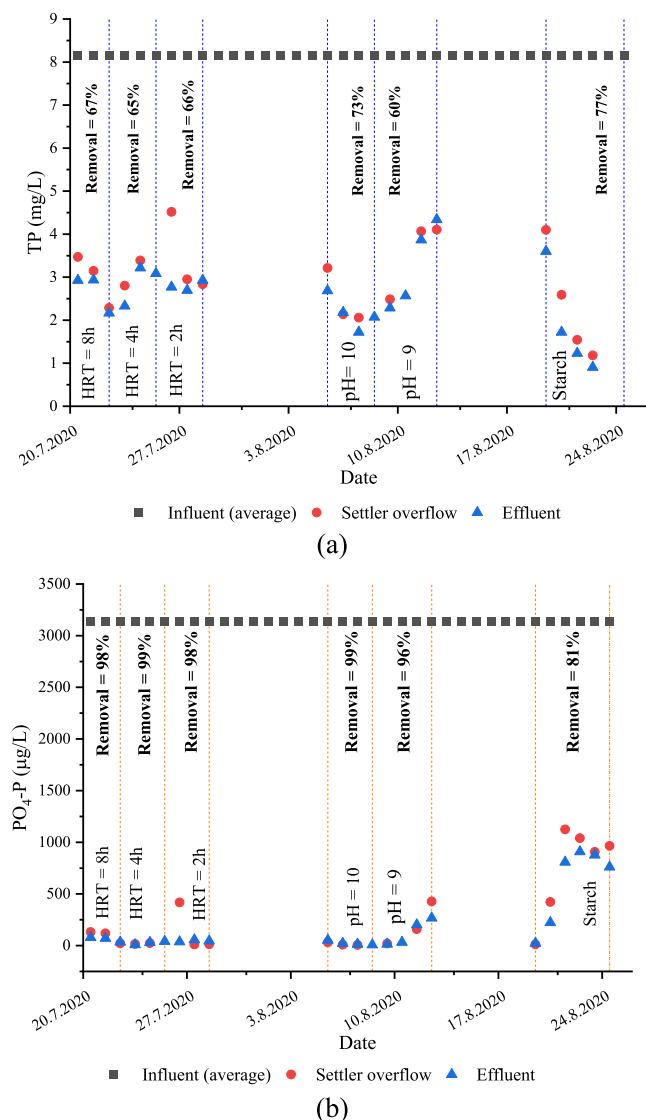


Fig. 12. Concentration profile and removal percentages of runs tested the effects of HRT, bulk pH, and pre-treatment type for (a) TP and (b) PO₄.

time in fast and slow mixing and consequently impacts P removal. In general, it seems that changing the HRT did not have a significant effect on P removal. It can be noticed that the TP profile resembles the SS profile for the same trials. This indicates that the mechanisms involved in solids removal are the same for total phosphorous, and this was also highlighted by another study on aquaculture wastewater [43]. The orthophosphate profile seems to follow the same trend as that of total phosphorus, except for the starch run. This suggests that starch is ineffective in removing this fraction of phosphorous.

With regards to the effect of varying treatment conditions, HRT seems to have an insignificant effect on TP and orthophosphate removal. Reducing pH from 10 to 9 reduced TP removal significantly, but it had a minor effect on PO₄³⁻ removal. Since TP removal follows the same mechanism as solids, this drop is logical as pH 9 resulted in lower solids removal compared to pH 10. Also, moving away from the optimum pH (pH 10 in this study) may lead to the particles' re-stabilization. Starch had higher TP removal than PAX, but PO₄³⁻ removal was lower. The possible mechanisms for phosphate removal with PAX are the formation of aluminum-hydroxo-phosphate complexes and the adsorption onto aluminum hydroxides formed at high pH [44,45]. It is also important to mention the effect of the polymer added with PAX. Polymers are likely to get attached to aluminum hydroxides, forming complexes and bridges

between particles. Consequently, phosphorous gets adsorbed onto the formed flocs through complexation and bridging mechanisms [46]. Superfloc A120 is an anionic polymer. This class of flocculants is known to contribute to particle removal through both bridging and charge neutralization mechanisms [47]. Charge neutralization is also responsible for P removal with starch [48]. Starch achieving higher removal of TP compared to PO₄³⁻ could be explained by the contribution of the enmeshment of the undissolved P fraction into the formed flocs. This could promote the formation of inorganic phosphorous salts with the scavenged metals from the bulk (e.g., Fe and Mg) (See Fig. S.7).

4.7. Characterization of P-containing sludge

The sludge formed in the process is an important product as it contains 65–77 % of the total phosphorous present in the water (see Fig. 12). Therefore, it is important to study the physical characteristics and chemical composition of the sludge. Since phosphorous removal is mainly affected by bulk pH and the pre-treatment type, only sludge from relevant runs was analyzed.

Sludge settleability of runs 2, 6, 7, and 10 for 30 min is shown in Fig. S.4. It is apparent that lowering the bulk pH negatively affected the settleability of the produced sludge. Both PAX/polymer and starch pre-treatments produced sludge with almost the same settleability pattern. The calculated cake resistance values are shown in Table 5. All treatments resulted in SVI₃₀ < 80 mL/g, which indicates that the sludge produced is dense and has high settleability [49]. The SVI₃₀ values obtained in this work are in the same range as those reported in recent studies [49,50].

Filterability tests were conducted to determine the cake resistance of the different sludge samples using Equation (16). Parameter *b* represents the slope resultant from plotting the inverse of sludge volume accumulation versus time for the filtration stage, as shown in Fig. S.5. The filtration stage can be differentiated from the compression stage by the change in the slope sharpness. As an example for demonstrating the filtration and compression stages, a dashed line was placed at the point that separates these two stages for PAX/polymer at pH 9. This line is different for PAX/polymer at the bulk pH of 10 and 11 as it occurs at a volume of 15 mL, and it is undetectable for starch within the volume range collected in the analysis. The calculated cake resistance values are shown in Table 4. Increasing the pH from 9 to 10 significantly improved the sludge filterability, indicated by both the lower cake resistance and extended filtration stage (Fig. S.5). However, a further increase in pH to 11 had an insignificant effect on cake resistance. The transition from filtration stage to compression stage stayed the same for pH 10 and pH 11, but the compression grew sharper for the former. These results show good agreement with the SS results presented in Fig. 2, where high solids removal was observed with bulk pH 10 in contrast to pH 9 and 11. Starch, on the other hand, had a significantly lower cake resistance than PAX/polymer in all treatment scenarios (20 times lower than PAX/polymer at the same bulk pH). This agrees with reported observations in the literature regarding the compatibility of sludge produced with starch [51]. In general, the obtained cake resistance values are in the same range as those reported in the literature for wastewater sludge [52]. As shown in Equation (16), the higher the value of *r*, the higher pressure required to filter and compress the sludge. This means that obtaining a low *r*-value is desirable, as it indicates a lower energy requirement for sludge dewaterability.

Table 5
Elemental analysis of sludge samples.

Elements	PAX/polymer sludge	Starch sludge
Nitrogen (%)	0.65	0.72
Hydrogen (%)	0.91	0.94
Carbon (%)	13.13	14.6

$$r = \frac{2A_f^2 Pb}{c \cdot \mu} \tag{16}$$

For further analysis of sludge quality, the metal content of the sludge samples for the treatments presented in Table 4 was also measured. The results are depicted in Fig. S.6. Note that metals with concentrations below 0.1 % were not reported in this figure for the sake of having a clear presentation. The dominant metal for all sludge samples is calcium with a percentage >80 %. The phosphorous content for the sludge produced from the PAX/polymer treatments was 0.7 %, and this figure was slightly higher for the starch treatment (0.8 %). This difference in P

percentage is due to the higher removal of starch and the difference in the chemical structure of the two coagulants. Starch is made mainly of atoms that are not detected by XRF (e.g., H, O, N, and C), while PAX is made of detectable metals (Al and Cl). Although this is a small percentage of P, it represents up to 77 % of P present in the rejected water. This small percentage is also considered reasonable given the amount of solids removed from the water and those added in the form of coagulants. Had the water contained more phosphorus, the sludge would have had a higher percentage of P, which would improve its value. Other metals with relatively high concentrations were Mg, Al, Si, S, and Fe. Metals with associated health concerns, such as Ni and Ti, were also

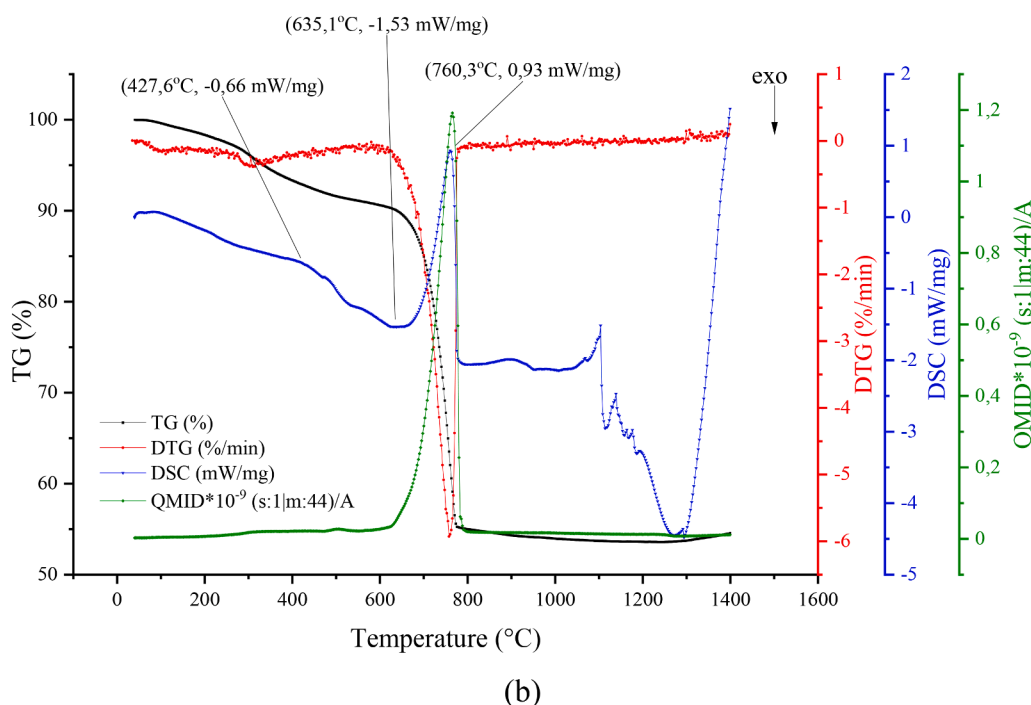
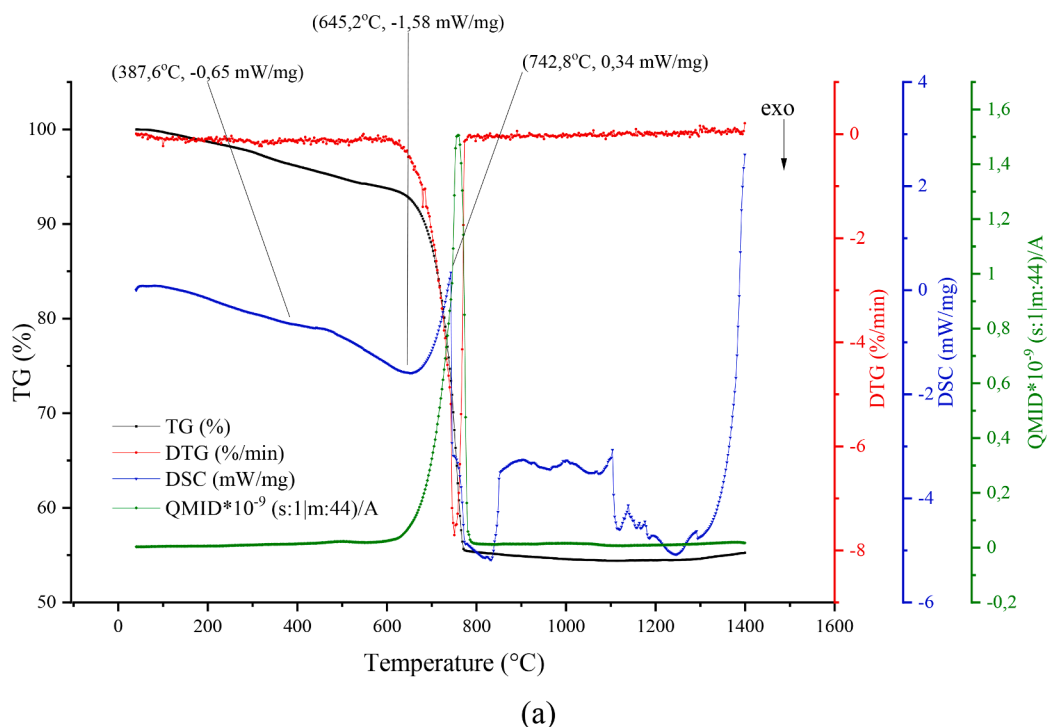


Fig. 13. TG-MS analysis of sludge samples: (a) PAX/polymer at pH 9, (b) PAX/polymer at pH 10, (c) PAX/polymer at pH 11, and (d) starch at pH 9.

present in the sludge, but at a negligible percentage range of 0.003–0.007 % and 0.03–0.06 %, respectively. The elemental analysis of sludge samples of the PAX/polymer treatment at pH 10 and the starch treatment at pH 9 is presented in Table 5. From an elemental analysis perspective, the sludge samples for both treatments were mainly made of carbon. These results confirm the XRF and XRD analyses that show that the sludge is encompassed mainly of calcium carbonate. The slightly higher carbon and nitrogen in starch sludge compared to PAX sludge makes sense, given the chemical composition of the two coagulants. The analysis presented here highlights the good quality of the produced sludge, which could be of use in agricultural applications if its phosphorus and nitrogen content is amended. The sludge can be used as is for acidic soil amendment due to its high calcium carbonate content [53].

A TG-MS analysis of the produced sludge with different slaked lime dosing and coagulants was also conducted. The results are illustrated in Fig. 13. In general, the weight loss curve (TG) for all the sludge samples, except bulk pH 9, exhibits two distinct regions—the first one in the temperature range of 200–450 °C and the second one above 600 °C. The TG curves observed in this study are similar to the reported TG curve patterns of sewage sludge observed in previous studies [54,55]. However, the reported weight loss regions in sewage sludge occurred in a lower temperature range of ≤ 180 °C for the first region and 180–580 °C for the second region. The first region is associated with the dehydration of the sample and the decomposition of simple and volatile carbon, while the second region signifies the destruction of complex carbon and inorganic constituents [56]. The high temperature required for the major weight reduction of the sludge sample is attributed to the presence of CaCO₃ in a very high percentage, as mentioned earlier. In fact, the sludge mass loss that occurred above 600 °C has mainly been reported to be ascribed to inorganic materials such as CaCO₃ [57]. Starch sludge left less ash than sludge produced with the PAX/polymer (weight loss of 50 % vs 45 %).

The other significant feature of the TG-MS analysis is the heat consumed and produced, indicated by DSC readings for endothermic and exothermic activities. The maximum weight loss of the starch sludge sample occurred at a lower temperature (615 °C) than that of PAX/polymer sludge (645 °C, 635 °C, and 642 °C for bulk pH of 9, 10, and 11, respectively). It is clear that the maximum weight loss is endothermic and required the specific energy of 0.34 mW/mg, 0.93 mW/mg, 0.23 mW/mg, and 0.40 mW/mg for sludge produced with PAX/polymer at pH 9, 10, 11, and starch, respectively. This suggests applying bulk pH 10 might have resulted in removing a high percentage of inorganic compounds that required high energy for decomposing them. The exothermic heat released from the decomposition of simple and volatile carbon (DSC curve dip at 600–650 °C) was higher for starch sludge than for PAX/polymer sludge. This can be explained by the carbonous structure of starch and its high capacity for volatile solids removal [27]. The changes in the DSC curve after around 800 °C are not believed to be due to the samples' structural change, as the weight is almost constant, and therefore they were ignored.

4.8. Quality evaluation of produced ammonium salts

Samples of 2 L of the obtained ammonium solutions with sulfuric and phosphoric acids were evaporated at 60 °C in the oven to produce ammonium salts for product quality analysis. Ammonium nitrate solution was not dried due to safety concerns associated with the explosive

Table 6
Elemental analysis of ammonium salts.

Elements	Ammonium sulfate	Ammonium phosphate
Nitrogen (%)	14.14	17.96
Hydrogen (%)	4.78	5.78
Sulfur (%)	27.13	14.26

nature of the dried salt. The elemental analysis of ammonium sulfate and ammonium phosphate salts is presented in Table 6. Note that the carbon content in the salt samples was zero, and thus it was removed from the table. The presence of sulfur in ammonium phosphate is due to the use of sulfuric acid to lower the pH to 3 to avoid ammonia loss during evaporation. The nitrogen content of ammonium sulfate obtained in this study is lower than that of commercial ammonium sulfate fertilizer (21 %), while the nitrogen content of ammonium phosphate is the same as that of commercial diammonium phosphates (18 %) [58]. This was addressed in earlier sections, as phosphoric acid has more capacity to absorb ammonia molecules compared to sulfuric acid. Note that the samples of the acids used for drying were taken from the experiments with diluted acids (0.5 M), which explains the low nitrogen content in both salts. Although the nitrogen content of ammonium phosphate suggests that the salt form is diammonium phosphate, an XRD analysis of the salt showed that the mono ammonium phosphate structure is prevalent, and the rest of the nitrogen is bound to sulfate (Fig. S.8). This agrees well with the pH measurements (Fig. S.2) and the proposed reaction pathway in Equation (14). For a pH range lower than 8, the likely structure formed is mono ammonium phosphate. Fig. S.8 also shows that ammonium sulfate is present in the crystal structures (NH₄)₃H(SO₄)₂ and NH₄HSO₄. The metal content in the produced ammonium salts was analyzed using XRF. The results are presented in Fig. S.9. Both salts have a high purity of approximately 99 %. There are some impurities represented by the presence of Ca, Si, Cl, and Zn. The presence of these elements can be explained by acids' impurities, cross-contamination during acid change, transport and storage, and measurement errors.

5. Conclusions

The upgraded NPHarvest system developed by our research team was tested for N and P recovery from mesophilic digester reject water at the Viikimäki WWTP. The effect of different operational parameters on N recovery and P removal was examined in a fully automated system under real industrial settings. The quality of the produced sludge and ammonium salts was also evaluated using advanced chemical analysis.

It was found that reducing the HRT significantly improved ammonia transfer across the membrane, resulting in a higher ammonia accumulation rate in the acid. Theoretical calculations proved that the improvement in ammonia transfer was due to the enhancement of the mass transfer constant and the reduction of the concentration polarization coefficient. Increasing the acid strength resulted in a lower ammonia accumulation rate. This is likely due to the drop in water activity on the lumen side and the increase in viscosity with high acid concentrations, which, in turn, hinders ammonia transfer across the membrane. It is recommended that the choice of acid strength should be based on the treatment process goal—whether it be nutrient removal or recovery. Out of the three bulk pH levels tested in this study, pH 10 seems to be the best pH level that resulted in the highest solids removal and, consequently, the highest ammonia recovery efficiency. When different acids were tested, nitric and sulfuric acid achieved almost the same ammonia accumulation rate, while the accumulation rate of phosphoric acid was lower than that of those two. This is attributed to the limited working pH range for phosphoric acid. Phosphoric acid dissociates to active species (e.g., HPO₄²⁻) at pH > 5, while ammonium conversion to ammonia starts taking place at pH ≥ 7 . Applying starch coagulation in the pre-treatment step had more or less the same ammonia recovery rate as that of PAX/polymer. However, the overall ammonia recovery efficiency was lower for starch than for PAX/polymer. Applying a lower mixing speed had an insignificant effect on ammonia recovery.

TP and orthophosphate profiles and removal figures were tracked for runs when bulk conditions were changed. TP followed the same pattern as solids, and its highest removal percentage was achieved with starch. Orthophosphate, on the other hand, was higher for bulk pH of 9. Bulk pH of 10 appears to be the optimum pH level for both N and P recovery.

Starch had a lower PO_4^{3-} removal than PAX/polymer.

The sludge produced with starch had better physical characteristics than that of PAX/polymer. Starch sludge has 20 times lower filtration cake resistance than PAX/polymer sludge. TG-MS and SVI_{30} analysis showed that the sludge produced from the pre-treatment step has characteristics similar to typical sewage sludge. A chemical analysis of sludge produced with PAX/polymer and starch shows that the sludge mainly consists of CaCO_3 and little amounts of other metals' salts such as Fe and Al. Despite the high P removal with the pre-treatment step, the sludge still has a low P content of 0.7–0.8%. This signifies the possibility of using the sludge as amendment material for acidic soil or supplementing its N and P content to make it more suitable for applications as fertilizer. The ammonium salts produced were of high purity. The nitrogen content of ammonium phosphate was the same as that of commercial fertilizer.

Further work on sludge quality improvement and its application in growth tests is required for future studies. Testing NPHarvest capacity for P recovery from WWTP with biological P removal would provide useful insights into the technology capability for implementation in a wider range of wastewater treatment processes. System design optimization for achieving minimal ammonia loss and high mass transfer rate is also needed for future improvement of the technology. The environmental impact of the NPHarvest system should also be investigated in future work. Developing systems for automated changing/replenishing of exhausted acids and concentrating the latter should be explored in the future.

CRedit authorship contribution statement

Raed A. Al-Juboori: Conceptualization, Methodology, Formal analysis, Investigation, Visualization, Supervision, Data curation, Writing – review & editing. **Juho Uzkuurt Kaljunen:** Conceptualization, Methodology, Investigation, Data curation, Resources, Software. **Ilaria Righetto:** Methodology, Investigation, Data curation, Resources, Software, Writing – original draft. **Anna Mikola:** Conceptualization, Supervision, Project administration, Funding acquisition.

Declaration of Competing Interest

The authors declare that they have no known competing financial interests or personal relationships that could have appeared to influence the work reported in this paper.

Acknowledgement

This study is part of the NPHarvest project, which was supported by the Ministry of Environment of Finland, RAKI2 project VN/2250/2019 and Maa- ja vesitekniiikan tuki r.y. (MVTT).

Appendix A. Supplementary data

Supplementary data to this article can be found online at <https://doi.org/10.1016/j.seppur.2022.122250>.

References

- [1] Food and Agriculture Organization of the United Nations, The Future of Food and Agriculture: Trends and Challenges, Rome, 2017, Available from: <https://www.fao.org/3/i6583e/i6583e.pdf>.
- [2] M.M. Damtie, F. Volpin, M. Yao, L.D. Tijng, R.H. Hailemariam, T. Bao, K.-D. Park, H.K. Shon, J.-S. Choi, Ammonia recovery from human urine as liquid fertilizers in hollow fiber membrane contactor: effects of permeate chemistry, *Environ. Eng. Res.* 26 (2020), 190523.
- [3] Y.V. Nancharaiyah, S. Venkata Mohan, P.N.L. Lens, Recent advances in nutrient removal and recovery in biological and bioelectrochemical systems, *Bioresour. Technol.* 215 (2016) 173–185, doi: 10.1016/j.biortech.2016.03.129.
- [4] R.W. Scholz, A.H. Roy, F.S. Brand, D.T. Hellums, A.E. Ulrich, Sustainable Phosphorus Management: A Global Transdisciplinary Roadmap, Springer, Netherlands, 2014 <https://books.google.fi/books?id=rdsBAAQBAJ>.
- [5] S.J. Van Kauwenbergh, World Phosphate Rock Reserves and Resources, International Fertilizer Development Center (IFDC), Alabama, USA, 2010.
- [6] G. Noriega-Hevia, J. Serralta, A. Seco, J. Ferrer, Economic analysis of the scale-up and implantation of a hollow fibre membrane contactor plant for nitrogen recovery in a full-scale wastewater treatment plant, *Sep. Purif. Technol.* 275 (2021), 119128, <https://doi.org/10.1016/j.seppur.2021.119128>.
- [7] Z. Guo, Y. Sun, S.-Y. Pan, P.-C. Chiang, Integration of green energy and advanced energy-efficient technologies for municipal wastewater treatment plants, *Int. J. Environ. Res. Public Health* 16 (2019) 1282, <https://doi.org/10.3390/ijerph16071282>.
- [8] N. Adouani, L. Limousy, T. Lendormi, O. Sire, N₂O and NO emissions during wastewater denitrification step: influence of temperature on the biological process, *C. R. Chim.* 18 (2015) 15–22, <https://doi.org/10.1016/j.crci.2014.11.005>.
- [9] R. Bashar, K. Gungor, K.G. Karthikeyan, P. Barak, Cost effectiveness of phosphorus removal processes in municipal wastewater treatment, *Chemosphere* 197 (2018) 280–290, <https://doi.org/10.1016/j.chemosphere.2017.12.169>.
- [10] B. Liu, A. Giannis, J. Zhang, V.-W.-C. Chang, J.-Y. Wang, Air stripping process for ammonia recovery from source-separated urine: modeling and optimization, *J. Chem. Technol. Biotechnol.* 90 (2015) 2208–2217, <https://doi.org/10.1002/jctb.4535>.
- [11] S.N. McCartney, N.A. Williams, C. Boo, X. Chen, N.Y. Yip, Novel isothermal membrane distillation with acidic collector for selective and energy-efficient recovery of ammonia from urine, *ACS Sustain. Chem. Eng.* 8 (2020) 7324–7334, <https://doi.org/10.1021/acssuschemeng.0c00643>.
- [12] H. Ray, F. Perreault, T.H. Boyer, Ammonia recovery from hydrolyzed human urine by forward osmosis with acidified draw solution, *Environ. Sci. Technol.* 54 (2020) 11556–11565, <https://doi.org/10.1021/acs.est.0c02751>.
- [13] C. Shin, A. Szczuka, R. Jiang, W.A. Mitch, C.S. Criddle, Optimization of reverse osmosis operational conditions to maximize ammonia removal from the effluent of an anaerobic membrane bioreactor, *Environ. Sci. Water Res. Technol.* 7 (2021) 739–747, <https://doi.org/10.1039/DOEW01112F>.
- [14] H. Wu, C. Vaneckhaute, Nutrient recovery from wastewater: a review on the integrated Physicochemical technologies of ammonia stripping, adsorption and struvite precipitation, *Chem. Eng. J.* (2021), 133664, <https://doi.org/10.1016/j.cej.2021.133664>.
- [15] J. Uzkuurt Kaljunen, R.A. Al-Juboori, A. Mikola, I. Righetto, I. Konola, Newly developed membrane contactor-based N and P recovery process: pilot-scale field experiments and cost analysis, *J. Clean. Prod.* 281 (2021) 125288, doi: 10.1016/j.jclepro.2020.125288.
- [16] M. Muys, R. Phukan, G. Brader, A. Samad, M. Moretti, B. Haiden, S. Pluchon, K. Roest, S.E. Vlaeminck, M. Spiller, A systematic comparison of commercially produced struvite: quantities, qualities and soil-maize phosphorus availability, *Sci. Total Environ.* 756 (2021), 143726, <https://doi.org/10.1016/j.scitotenv.2020.143726>.
- [17] S. Astals, M. Martínez-Martorell, S. Huete-Hernández, V.B. Aguilar-Pozo, J. Dosta, J.M. Chimenos, Nitrogen recovery from pig slurry by struvite precipitation using a low-cost magnesium oxide, *Sci. Total Environ.* 768 (2021), 144284, <https://doi.org/10.1016/j.scitotenv.2020.144284>.
- [18] M. Darestani, V. Haigh, S.J. Couperthwaite, G.J. Millar, L.D. Nghiem, Hollow fibre membrane contactors for ammonia recovery: current status and future developments, *J. Environ. Chem. Eng.* 5 (2017) 1349–1359.
- [19] J. Zhang, M. Xie, X. Tong, D. Yang, S. Liu, D. Qu, L. Feng, L. Zhang, Ammonia capture from human urine to harvest liquid N-P compound fertilizer by a submerged hollow fiber membrane contactor: performance and fertilizer analysis, *Sci. Total Environ.* 768 (2021), 144478, <https://doi.org/10.1016/j.scitotenv.2020.144478>.
- [20] J. Zhang, M. Xie, X. Tong, S. Liu, D. Qu, S. Xiao, Recovery of ammonium nitrogen from human urine by an open-loop hollow fiber membrane contactor, *Sep. Purif. Technol.* 239 (2020), 116579, <https://doi.org/10.1016/j.seppur.2020.116579>.
- [21] Helsinki Region Environmental Services Authority (HSY), Jätevedenpuhdistus pääkaupunkiseudulla 2018: Viikinnäen ja Suomenojan jätevedenpuhdistamot, 2019, Available from: <https://julkaisu.hsy.fi/jatevedenpuhdistus-paakaupunkiseudulla-2018.pdf> (accessed September 22, 2021).
- [22] I. Righetto, R.A. Al-Juboori, J.U. Kaljunen, A. Mikola, Wastewater treatment with starch-based coagulants for nutrient recovery purposes: testing on lab and pilot scales, *J. Environ. Manage.* 284 (2021), <https://doi.org/10.1016/j.jenvman.2021.112021>.
- [23] R. Sah, Development and optimization of pilot plant for nutrient recovery from reject water, 2019, Available from: <https://aaltoodoc.aalto.fi/handle/123456789/37940>.
- [24] I. Righetto, R.A. Al-Juboori, J.U. Kaljunen, N. Huynh, A. Mikola, Nitrogen recovery from landfill leachate using lab-and pilot-scale membrane contactors: research into fouling development and membrane characterization effects, *Membranes* 12 (2022) 837.
- [25] E.W. Rice, R.B. Baird, A.D. Eaton, L.S. Clesceri, Standard Methods for the Examination of Water and Wastewater, 23rd ed., American Public Health Association, Washington, DC, 2017.
- [26] A. Eaton, L.S. Clesceri, E.W. Rice, A.E. Greenberg, M.J.C.E. Franson, Standard Methods for the Examination of Water and Wastewater, 21st ed., American Water Works Association (AWWA) & Water Environment Federation (WEF), Washington, DC, 2005.
- [27] I. Righetto, R.A. Al-Juboori, J.U. Kaljunen, A. Mikola, Wastewater treatment with starch-based coagulants for nutrient recovery purposes: testing on lab and pilot scales, *J. Environ. Manage.* 284 (2021), 112021, <https://doi.org/10.1016/j.jenvman.2021.112021>.

- [28] S. Jiahui, F. Xuliang, H.E. Yiliang, J.L.N. Qiang, Emergency membrane contactor based absorption system for ammonia leaks in water treatment plants, *J. Environ. Sci.* 20 (2008) 1189–1194.
- [29] M. Khayet, Membranes and theoretical modeling of membrane distillation: a review, *Adv. Colloid Interface Sci.* 164 (2011) 56–88, <https://doi.org/10.1016/j.cis.2010.09.005>.
- [30] M. Khayet, T. Matsuura, *Membrane Distillation: Principles and Applications*, Elsevier, 2011.
- [31] O. Miyawaki, A. Saito, T. Matsuo, K. Nakamura, Activity and activity coefficient of water in aqueous solutions and their relationships with solution structure parameters, *Biosci. Biotechnol. Biochem.* 61 (1997) 466–469, <https://doi.org/10.1271/bbb.61.466>.
- [32] S.N. Ashrafizadeh, Z. Khorasani, Ammonia removal from aqueous solutions using hollow-fiber membrane contactors, *Chem. Eng. J.* 162 (2010) 242–249, <https://doi.org/10.1016/j.cej.2010.05.036>.
- [33] G. Noriega-Hevia, J. Serralta, L. Borrás, A. Seco, J. Ferrer, Nitrogen recovery using a membrane contactor: modelling nitrogen and pH evolution, *J. Environ. Chem. Eng.* 8 (2020), 103880, <https://doi.org/10.1016/j.jece.2020.103880>.
- [34] A. Hasanoglu, J. Romero, B. Pérez, A. Plaza, Ammonia removal from wastewater streams through membrane contactors: experimental and theoretical analysis of operation parameters and configuration, *Chem. Eng. J.* 160 (2010) 530–537, <https://doi.org/10.1016/j.cej.2010.03.064>.
- [35] M.A. Boehler, A. Heisele, A. Seyfried, M. Grömping, H. Siegrist, (NH₄)₂SO₄ recovery from liquid side streams, *Environ. Sci. Pollut. Res.* 22 (2015) 7295–7305, <https://doi.org/10.1007/s11356-014-3392-8>.
- [36] S. Shen, S.E. Kentish, G.W. Stevens, Shell-side mass-transfer performance in hollow-fiber membrane contactors, solvent extraction and ion, *Exchange* 28 (2010) 817–844, <https://doi.org/10.1080/07366299.2010.515176>.
- [37] L. Chen, C.-D. Ho, L.-Y. Jen, J.-W. Lim, Y.-H. Chen, Augmenting CO₂ absorption flux through a gas-liquid membrane module by inserting carbon-fiber spacers, *Membranes* 10 (2020) 302, <https://doi.org/10.3390/membranes10110302>.
- [38] R.A. Johnson, M.H. Nguyen, *Understanding Membrane Distillation and Osmotic Distillation*, John Wiley & Sons, 2017.
- [39] S. Ortakci, H. Yesil, A.E. Tugtas, Ammonia removal from chicken manure digestate through vapor pressure membrane contactor (VPMC) and phytoremediation, *Waste Manage.* 85 (2019) 186–194, <https://doi.org/10.1016/j.wasman.2018.12.033>.
- [40] E. Reyhanitash, B. Zaalberg, S.R.A. Kersten, B. Schuur, Extraction of volatile fatty acids from fermented wastewater, *Sep. Purif. Technol.* 161 (2016) 61–68, <https://doi.org/10.1016/j.seppur.2016.01.037>.
- [41] A. Limoli, M. Langone, G. Andreottola, Ammonia removal from raw manure digestate by means of a turbulent mixing stripping process, *J. Environ. Manage.* 176 (2016) 1–10, <https://doi.org/10.1016/j.jenvman.2016.03.007>.
- [42] P. Brezonik, W. Arnold, *Water Chemistry: An Introduction to the Chemistry of Natural and Engineered Aquatic Systems*, Oxford University Press, 2011.
- [43] J.M. Ebeling, P.L. Sibrell, S.R. Ogden, S.T. Summerfelt, Evaluation of chemical coagulation–flocculation aids for the removal of suspended solids and phosphorus from intensive recirculating aquaculture effluent discharge, *Aquacult. Eng.* 29 (2003) 23–42, [https://doi.org/10.1016/S0144-8609\(03\)00029-3](https://doi.org/10.1016/S0144-8609(03)00029-3).
- [44] K.C.D.V. Gamage, *Removal of Phosphorus from Municipal Wastewater*, Curtin University, 2016.
- [45] L.D. Manamperuma, H.C. Ratnaweera, A. Martsul, Mechanisms during suspended solids and phosphate concentration variations in wastewater coagulation process, *Environ. Technol.* 37 (2016) 2405–2413.
- [46] M. Özacar, İ.A. Şengil, Enhancing phosphate removal from wastewater by using polyelectrolytes and clay injection, *J. Hazard. Mater.* 100 (2003) 131–146, [https://doi.org/10.1016/S0304-3894\(03\)00070-0](https://doi.org/10.1016/S0304-3894(03)00070-0).
- [47] W.A. Shewa, M. Dagne, Revisiting chemically enhanced primary treatment of wastewater: a review, *Sustainability* 12 (2020) 5928, <https://doi.org/10.3390/su12155928>.
- [48] Y. Tang, X. Hu, J. Cai, Z. Xi, H. Yang, An enhanced coagulation using a starch-based coagulant assisted by polysilicic acid in treating simulated and real surface water, *Chemosphere* 259 (2020), 127464, <https://doi.org/10.1016/j.chemosphere.2020.127464>.
- [49] M.I. Ejimofor, I.G. Ezemagu, M.C. Menkiti, Physicochemical, Instrumental and thermal characterization of the post coagulation sludge from paint industrial wastewater treatment, *South African. J. Chem. Eng.* 37 (2021) 150–160, <https://doi.org/10.1016/j.sajce.2021.05.008>.
- [50] T. Jaouadi, M. Hajji, M. Kasmi, A. Kallel, A. Chatti, H. Hamzaoui, A. Mnif, C. Tizaoui, I. Trabelsi, Aloe sp. leaf gel and water glass for municipal wastewater sludge treatment and odour removal, *Water Sci. Technol.* 81 (2020) 479–490, <https://doi.org/10.2166/wst.2020.123>.
- [51] N.A. Oladoja, Headway on natural polymeric coagulants in water and wastewater treatment operations, *J. Water Process Eng.* 6 (2015) 174–192, <https://doi.org/10.1016/j.jwpe.2015.04.004>.
- [52] Y. Qi, K.B. Thapa, A.F.A. Hoadley, Application of filtration aids for improving sludge dewatering properties – a review, *Chem. Eng. J.* 171 (2011) 373–384, <https://doi.org/10.1016/j.cej.2011.04.060>.
- [53] R. Chintala, J. Mollinedo, T.E. Schumacher, D.D. Malo, J.L. Julson, Effect of biochar on chemical properties of acidic soil, *Arch. Agronomy Soil Sci.* 60 (2014) 393–404, <https://doi.org/10.1080/03650340.2013.789870>.
- [54] A. Magdziarz, S. Werle, Analysis of the combustion and pyrolysis of dried sewage sludge by TGA and MS, *Waste Manage.* 34 (2014) 174–179, <https://doi.org/10.1016/j.wasman.2013.10.033>.
- [55] A. Magdziarz, M. Wilk, Thermal characteristics of the combustion process of biomass and sewage sludge, *J. Therm. Anal. Calorim.* 114 (2013) 519–529, <https://doi.org/10.1007/s10973-012-2933-y>.
- [56] S. Verma, B. Prasad, I.M. Mishra, Pretreatment of petrochemical wastewater by coagulation and flocculation and the sludge characteristics, *J. Hazard. Mater.* 178 (2010) 1055–1064, <https://doi.org/10.1016/j.jhazmat.2010.02.047>.
- [57] L. Kubonova, I. Janakova, P. Malikova, S. Drabinova, M. Dej, R. Smelik, P. Skalny, S. Heviankova, Evaluation of waste blends with sewage sludge as a potential material input for pyrolysis, *Appl. Sci.* 11 (2021) 1610, <https://doi.org/10.3390/app11041610>.
- [58] European Commission, *Fertilisers in the EU: prices, trade and use*, Agriculture and Rural Development, 2019, Available from: https://ec.europa.eu/info/sites/default/files/food-farming-fisheries/farming/documents/market-brief-fertilisers_june2019_en.pdf (accessed September 11, 2021).